A SEARCH FOR THE STANDARD MODEL HIGGS DECAYING TO TWO MUONS AT THE CMS EXPERIMENT

By

ANDREW CARNES

A DISSERTATION PRESENTED TO THE GRADUATE SCHOOL
OF THE UNIVERSITY OF FLORIDA IN PARTIAL FULFILLMENT
OF THE REQUIREMENTS FOR THE DEGREE OF
DOCTOR OF PHILOSOPHY

UNIVERSITY OF FLORIDA

2017

ACKNOWLEDGMENTS

I would like to thank my Mom and Dad for just being all around great parents. Without all of their support, the completion of this Ph.D would never have been possible. I would also like to thank Professors Paul Avery and Darin Acosta for their help. In addition, I would like to thank Andrew Brinkerhoff, Pierluigi Bortignon, and Andrea Marini for all of their support and hard work on the project. I'd also like to thank my friends Stany, Leo, Sean, Sophie, and David for making Geneva a great place to live.

TABLE OF CONTENTS

LIST OF TABLES

Table page

LIST OF FIGURES

Abstract of Dissertation Presented to the Graduate School
of the University of Florida in Partial Fulfillment of the
Requirements for the Degree of Doctor of Philosophy

A SEARCH FOR THE STANDARD MODEL HIGGS DECAYING TO TWO MUONS AT THE CMS EXPERIMENT

By

Andrew Carnes

December 2017

Chair: Paul Avery
Major: Physics

In 2012 two collaborations at the Large Hadron Collider announced the discovery of a new particle with properties similar to the Standard Model Higgs Boson. In order to determine whether the boson discovered with a mass of 125 GeV is actually the Standard Model Higgs, all of the different ways the particle can decay need to be investigated. If the probabilities for the different decays do not match the predictions of the Standard Model then this would imply new physics.

This dissertation presents the search for the Standard Model Higgs Boson decaying to $\mu^+\mu^-$. The search uses the 35.9 ± 0.9 fb^{-1} of $\sqrt{s} = 13$ TeV proton-proton collision data recorded by the CMS detector in 2016. The observed and expected upper limits on the rate at a 95 % confidence level are presented for Higgs masses in the range 120 to 130 GeV. The expected and observed upper limits at a mass of 125 GeV are x.xx and $1.98^{+0.81}_{-0.57} \times$ SM respectively. These results provide the best results to date on the Higgs coupling to second generation fermions. No deviations from the Standard Model are observed.

CHAPTER 1
INTRODUCTION

The Standard Model of particle physics is an extremely successful theory shown to correctly predict the behavior of the particles and forces which make up the most basic constituents of the universe. In fact, it correctly describes all of the forces known except for gravity. All of the elementary particles detailed in the Standard Model have been discovered except for one, the Higgs boson. As explained by special relativity, potential energy can be realized as mass and it is the potential from the interaction with the nonzero Higgs field that bestows mass onto the massive elementary particles in the Standard Model. On July 4, 2012 two collaborations at the Large Hadron Collider (LHC), the A Toroidal LHC Apparatus (ATLAS) and Compact Muon Solenoid (CMS), announced the discovery of a new boson at 125 GeV with properties similar to the Standard Model Higgs **???**. This discovery was fueled by the investigation into the Higgs decays to the vector bosons ZZ and $\gamma\gamma$. Soon after, evidence for the Higgs coupling to matter was found through the $\tau^+\tau-$ and $\mathrm{b\bar{b}}$ decays **????**. Whether the newly discovered boson is indeed the expected Standard Model Higgs remains to be determined. Insofar, all of the different decay modes will be investigated to search for deviations from the Standard Model predictions.

This leads to the study of the Higgs decay to $\mu^+\mu^-$. Although this decay is the smallest branching fraction expected to be detected **??**, the dimuon decay offers high efficiency and excellent momentum resolution, which should lead to a narrow peak over the falling background, mostly Drell Yan events. The tiny branching fraction enables greater sensitivity to small deviations from the predicted decay rate and in this respect offers an advantage over other channels where a miniscule deviation could be drowned out. Furthermore, the Higgs coupling to second generation fermions remains to be determined.

This dissertation presents the search for the Standard Model Higgs Boson decaying to $\mu^+\mu^-$ using the proton-proton collision data recorded by the CMS experiment in 2016. In order to maximize the data available for the search, the first machine learning in the L1 Trigger

system at the LHC was developed and deployed for 2016 data collection. To further maximize the sensitivity of the search, an additional machine learning technique is invented to categorize events based upon the detector resolution and the event kinematics. The search looks for a Higgs boson with a mass between 120 and 130 GeV and presents the expected and observed upper limits in this range.

The dissertation first presents an overview of the Standard Model and the symmetry breaking mechanism within the theory responsible for the Higgs. After covering the theoretical basis for the Standard Model Higgs, the accelerating apparatus responsible for accelerating and colliding the protons, the LHC, is covered. Then the CMS detector responsible for measuring the paths, momentum, and energy of the particles emerging from every collision is reviewed. Next the machine learning implementation in the L1 trigger that enables the detector to save more of the relevant collisions data is detailed. After, the search for H to $\mu^+\mu^-$ is presented and then finally the conclusions.

CHAPTER 2
THE LARGE HADRON COLLIDER AND THE CMS EXPERIMENT

2.1 Large Hadron Collider

The Large Hadron Collider is a particle collider near Geneva, Switzerland run by the European Organization for Nuclear Research (CERN). The LHC is the largest and most powerful particle collider ever built, designed to collide protons with a center of mass energy of 14 TeV and a luminosity of $10^{34}\mathrm{cm}^{-2}\mathrm{s}^{-1}$ **?**. The luminosity is given by

$$\mathrm{L} = \frac{\mathrm{n_b f N_p^2 \gamma}}{4\pi\epsilon_\mathrm{n}\beta^*} \tag{2–1}$$

where $\mathrm{n_b}$ is the number of bunches in each ring, f is the frequency for a bunch to circle the ring, $\mathrm{N_p}$ gives the number of protons in a bunch, and γ is the Lorentz factor. ϵ_n is the normalized transverse emittance, a measure of the spread of the beam in momentum and position space. β^* measures the focus of the beam at the interaction point. $\epsilon_\mathrm{n}\beta^*$ represents the transverse area at the point of interaction. A large luminosity is characterized by a high frequency of bunch crossings with lots of protons in each bunch packed as densely as possible, and a large luminosity results in a high rate of collisions. With many collisions at high energy, the detectors can collect enough events from yet unexplored regimes of physics to discover new physics or to verify or discard the predictions different hypothesis, so these parameters are very important.

The collider itself is 26.7 km in circumference 45-170 m underground. 8.3 T supercooled superconducting magnets operating at 2 K steer the high energy proton beams. In order to save money the LHC not only reuses the tunnels of a previous collider, the Large Electron Positron Collider (LEP), but also reuses older accelerators which were state of the art at their time. These older accelerators ramp up the energy of the protons and inject them into the LHC. All of this together makes up the CERN accelerator complex.

First, the protons are created from a source of Hydrogen gas. The hydrogen atoms of the gas are placed into a large electric field that separates the atoms into unbound protons

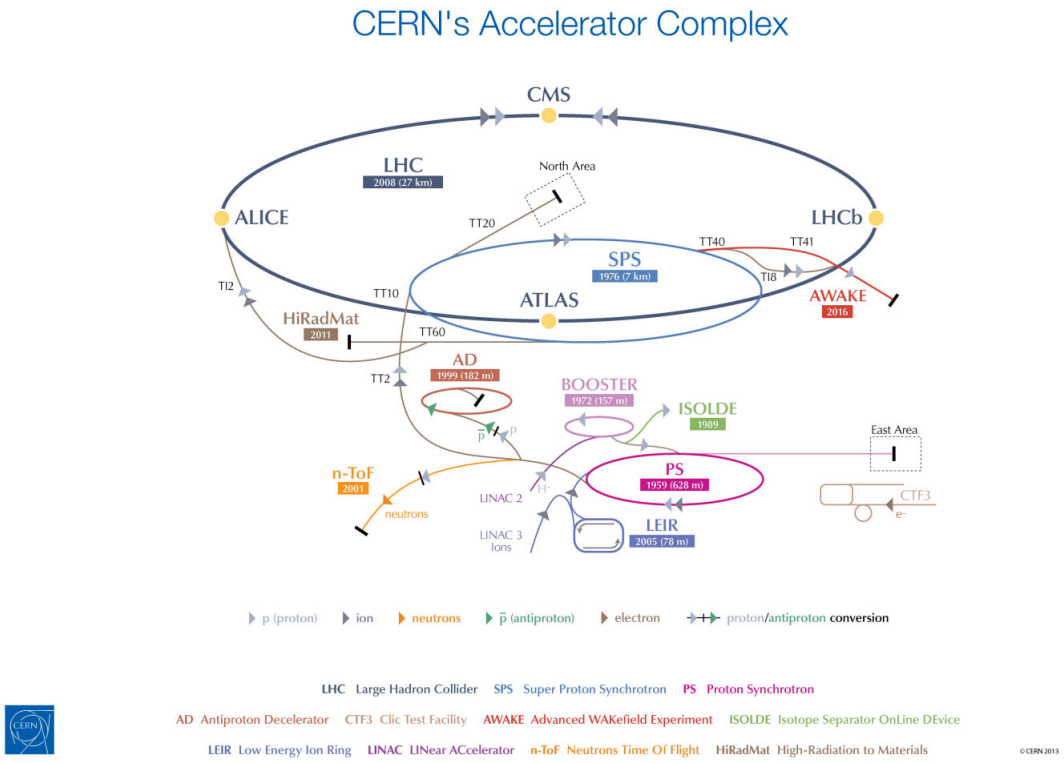

Figure 2-1. The CERN Accelerator Complex **?**

and electrons. The protons are then sent to a radio frequency quadrapole which focuses the protons and accelerates them. The radio frequency field is stronger for the protons in the back than in the front and consequently squeezes them into a tighter bunch. The protons then proceed to a linear accelerator, LINAC2, where they are accelerated to 50 MeV or 5% of the speed of light (c). The protons then enter a series of synchrotrons. A synchrotron is a device that accelerates particles by guiding them around a fixed circular path with a magnetic field and boosting their speed with an electric field as they pass a certain point. Since a faster particle bends less in the same magnetic field, the magnetic field strength is synchronized with the speed of the accelerating particles to keep them in the fixed circular path.

After LINAC2 the protons enter the first of the synchrotrons, the Proton Synchrotron Booster (PSB) accelerating the protons to 1.4 GeV (0.81c). From here the protons are injected into the Proton Synchrotron (PS) and accelerate to 25 GeV (0.999c). The PS then injects

the protons into the Super Proton Synchrotron (SPS) further accelerating them to 450 GeV (0.99999c). Finally the protons are injected into the LHC where they accelerate up to 6.5 TeV (0.99999999c). Once accelerated to the appropriate collision energy, the proton beams are made to collide in the different detectors located around the ring. By colliding enough protons at large enough energies it is possible to probe corners of physics that have never been seen before. The two general purpose detectors at the LHC, ALTAS and CMS, are used to look for signs of new physics like the Higgs boson, dark matter, and extra dimensions by measuring the energy, the momentum, and the paths of the particles coming out of the collisions.

2.2 Compact Muon Solenoid Detector

The CMS detector, located in Cessy, France, is 21.6 m long, 15 m in diamater, and weighs more than the Eiffel Tower. Not only is the detector a massive and complex device it's also run by a huge collaboration involving approximately 3,800 people from 200 institutes spanning 43 different countries **?**. The greatest achievement of the collaboration to date is the discovery of a Higgs like particle in 2012, a feat shared with ATLAS.

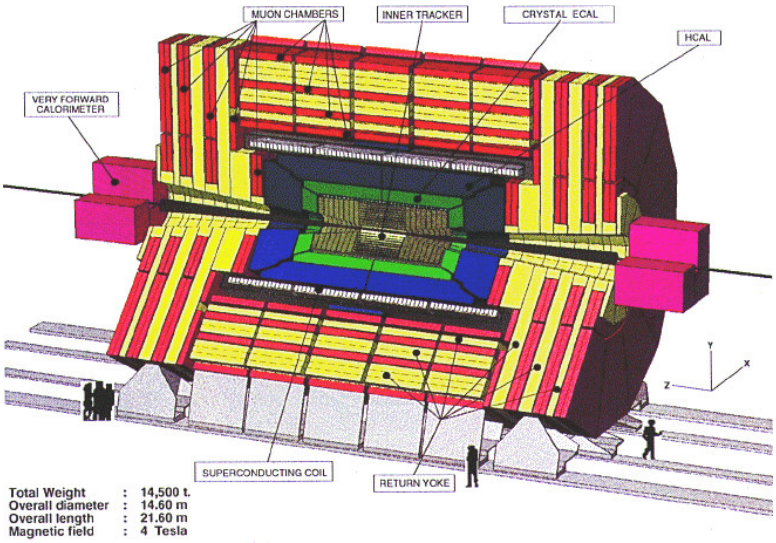

Figure 2-2. The CMS detector **?**

CMS was built primarily to look for the Standard Model Higgs and signs of Beyond Standard Model (BSM) physics like Supersymmetry, extra dimensions, or new heavy weak bosons **?**. Because BSM and Higgs decays to muons and electrons often have the highest

signal to background ratio, CMS is designed to identify and measure these particles with a high accuracy. In layman's terms a high signal to background ratio just means that these events have fewer look-alikes. Jets [1] and photons are measured to a high degree of accuracy as well. In order to measure the energy, momentum, and location of the different types of particles CMS deploys a variety of subdetectors working in concert. The defining feature of the detector is an extremely powerful solenoid which enables the accurate measurement of momentum for charged particles. The tracker and calorimeters fit snugly within the 6 m diameter solenoid. The muon detectors reside outside the magnet but within the return yoke.

2.2.1 Silicon Tracker

The 3.8T magnetic field inside the solenoid enables the tracker to measure the transverse momentum of charged particles based upon the curvature of the track. Charged particles with lower transverse momentum ($\mathrm{p_t}$) bend more in a magnetic field than high $\mathrm{p_t}$ particles. As such, a measurement of the deviation of a curved track from a straight line, the sagitta, can be used to measure the curvature and determine the momentum **?**.

$$\mathrm{p_t} \cong \frac{\mathrm{L^2 qB}}{8\mathrm{s}} \tag{2–2}$$

Here L is the length of the straight line between the first and last position measurments, q is the charge of the particle, B is the magnetic field, and s is the sagitta.

The equation for the error in the momentum measurement shows that a higher magnetic field enables better $\mathrm{p_t}$ resolution, illuminating the design choice for a powerful magnet.

$$\frac{\delta \mathrm{p_t}}{\mathrm{p_t}} \propto \frac{\mathrm{p_t}}{\mathrm{L^2 B}} \tag{2–3}$$

[1] When a quark or gluon is created it can't exist alone, since it has color charge, and pulls other quarks from the vacuum creating a tight cone of composite colorless particles as well as their decays. This cone of particles is called a jet.

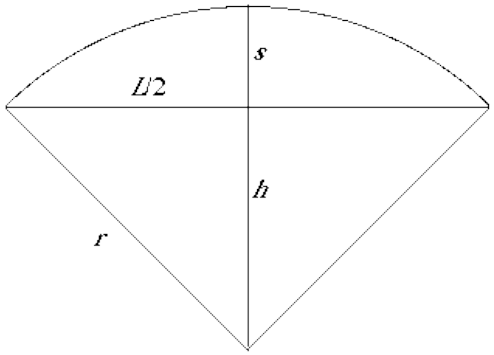

Figure 2-3. The sagitta measurement

The silicon tracker is made of tiny reverse biased bipolar diodes. When a charged particle travels through one of these diodes the ionization force of the particle releases electron hole pairs beyond the electrostatic equilibrium, inciting a current to flow. The tracker needs to be small enough such that the particles flowing through it don't deposit much energy. Energy deposition in the tracker would throw off energy measurements in the calorimeters. This means that the tracker needs to be smaller than a few radiation lengths [2] . The tracker at the thickest part is one radiation length. The tracker is placed nearest the collision point in order to identify primary and secondary vertices and to measure the momentum of particles before they are tainted by interactions with other detectors. [3] Being so near the collision point, the silicon tracker is bombarded by a constant flux of high intensity radiation. As such, the tracker is carefully designed to be robust to this radiation rich environment.

2.2.2 Calorimeters

The Electromagnetic Calorimeter (ECAL) is right outside the tracker and its main goal is to measure the energy of electrons and photons. It's designed to contain entire electromagnetic

[2] the length scale over which an electron deposits a substantial amount of energy into the material

[3] Vertex is shorthand for the location of the collision or decay that produced a set of particles.

showers for these particles and is consequently many radiation lengths thick. The ECAL is made of lead tungstenate scintillating crystals which release an amount of light proportional to the energy deposition. The light is collected and the total energy is calculated. The separation into individual crystals allows some spatial resolution as well. Particles with larger mass deposit less energy per unit distance into a solid. Many of the hadronic particles make it through the ECAL for this reason.

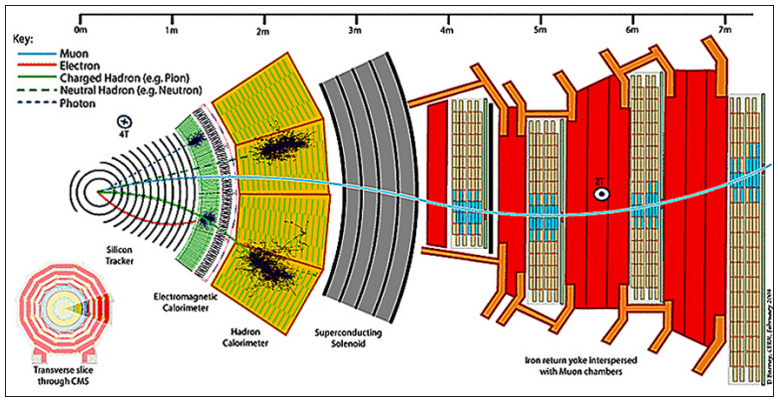

Figure 2-4. A slice of the CMS detector **?**

The HCAL is placed outside the ECAL to collect the energy of the particles that survived the other subsystems, mostly strongly interacting hadronic particles from jets. The HCAL works in a similar manner to the ECAL except that layers of plastic scintillating material are interspersed with layers of a dense passive absorber like brass or steel. The density of the passive absorber increases the chance of interaction and shower production thus reducing the total length of the hadronic shower and enabling the measurement of the total energy for most of the cascades. Again the scintillation light is collected to determine the energy. If the ECAL and HCAL were placed outside the magnet the particles would interact with the solenoid material before entering the calorimeters, throwing off their measurements. The showers in the calorimeters are a consequence of the electromagnetic and strong forces, which means that particles without these interactions pass through the materials undetected, e.g. neutrinos or BSM weakly interacting particles. Since the momentum in an interaction is conserved any imbalance means that some particles escaped the detector. If there is an excess of missing

momentum beyond the amount expected due to neutrinos this may indicate the existence of dark matter or some other BSM particle. In order to measure the missing energy correctly it's important that the HCAL is built without any gaps and that it is dense enough to collect the energy of the strongly and electrically interacting particles.

While the momentum resolution in the tracker is proportional to the momentum, the energy resolution in the calorimeters decreases with increasing energy **?**.

$$\frac{\delta \mathrm{E}}{\mathrm{E}} = \sqrt{\left(\frac{\mathrm{S}}{\sqrt{\mathrm{E}}}\right)^2 + \left(\frac{\mathrm{N}}{\mathrm{E}}\right)^2 + \mathrm{C}} \tag{2–4}$$

The first term in the square root describes statistical fluctuations. The energy measured is proportional to the number of photons captured which has poisonnian fluctuations and the error ($\delta \mathrm{E}$) for this term is $\propto \sqrt{\mathrm{E}}$. The second term describes noise in the electronics whose error is energy independent, and the last term describes the errors in energy calibration which are proportional to energy.

2.2.3 Muon System

Neutrinos aren't the only Standard Model particles that make it through the tracker, ECAL, and HCAL. Muons have a relatively long lifetime $\sim 10^{-6}\mathrm{s}$ with $\mathrm{c}\tau \sim 100\mathrm{m}$. The large gamma factor in combination with their long lifetime enables them to travel hundreds of kilometers on average, well through the entire CMS detector before decaying. Muons are charged so their tracks show up in the tracker and some energy is deposited in the calorimeters but, muons are so much more massive than electrons that the energy deposition in the ECAL is minimal. Making it through the ECAL the muons enter the HCAL. The HCAL is designed to stop strongly interacting hadronic particles and collect their energy. But muons don't interact with the strong force and make it through the HCAL as well. This enables the muon system to be placed outside the magnet.

The muon system consists of a few different types of detectors which all involve the same basic principle. The charged muon ionizes some gas and the ionized particles are attracted to charged surfaces initiating a current in the surfaces. With a large enough voltage differential

between the charged surfaces the the ionized particles may gain enough kinetic energy to further ionize other atoms in the gas initiating an avalanche effect and reducing the need for signal amplification later. The muon system uses this strategy in the different detectors. The types of detectors in the muon system are the Cathode Strip Chambers (CSC), the Drift Tubes (DT), and the Resistive Plate Chambers (RPC) **?**.

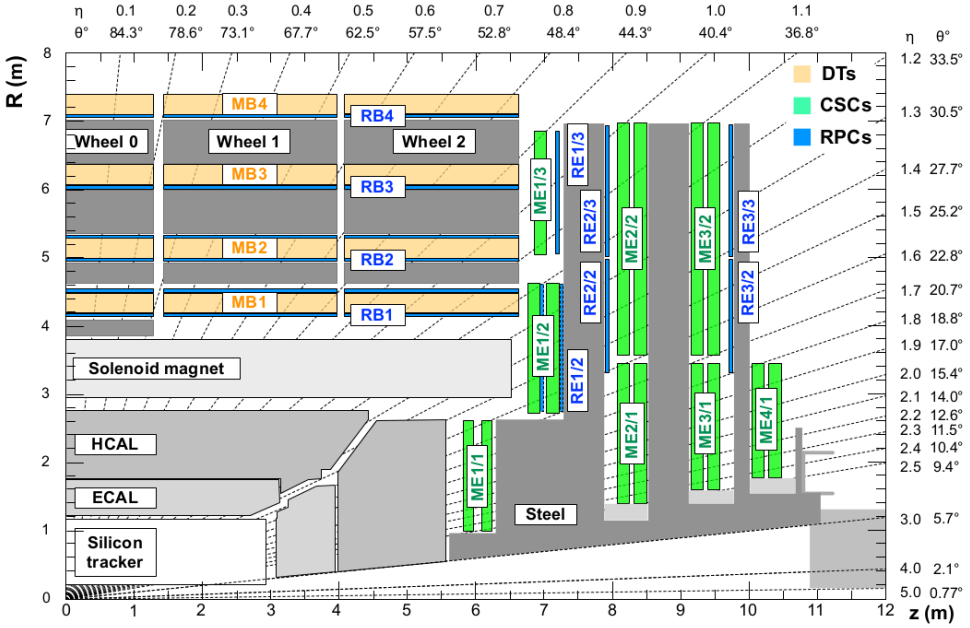

Figure 2-5. A Look at the Muon System **?**

2.2.3.1 Drift Tubes

The drift tubes are located in the barrel portion of CMS. Throughout the majority of the barrel the magnetic field is basically uniform. The drift tubes have aluminum plates on the top and bottom separated by aluminum I-beams shown in Figure 2-6. A wire acts as the anode and the I-beams are the cathodes. The tubes are designed to provide a constant drift velocity throughout each tube.

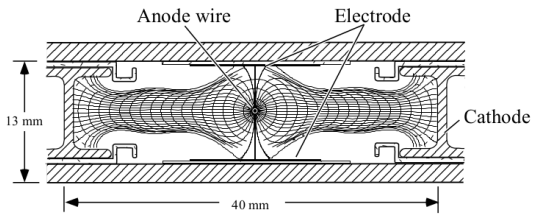

Figure 2-6. A Drift Tube **?**

When a charged particle flies through the tube it ionizes the gas inside. The electrons drift at constant velocity to the anode. The distance from the anode is deduced from the drift time, utilizing the fact that the ionized electrons drift with a constant velocity. This calculation does however require a reference time. In each chamber the drift tubes are placed in layers and the average crossing time in the chamber is used as the reference time.

2.2.3.2 Cathode Strip Chambers

The CSCs are located in the endcaps of the detector which range in $|\eta|$ from 0.8 to 2.4. One of the reasons the endcaps use CSCs instead of DTs is the nonuniform magnetic field which would adversely affect the drift times in the DT system. In this system there are oppositely charged strips and wires running roughly perpendicular to eachother.

When a muon flies through the CSC it induces charge on the wires and the strips and ionizes gas in the chamber. The ionized particles in the gas float to the charged strips and wires initiating a current in the nearby wires and strips. The induced charge from the muon itself also contributes to the currents. The most intense currents should be those associated with the location of the muon. The position resolution in the phi direction is roughly 100 μm.

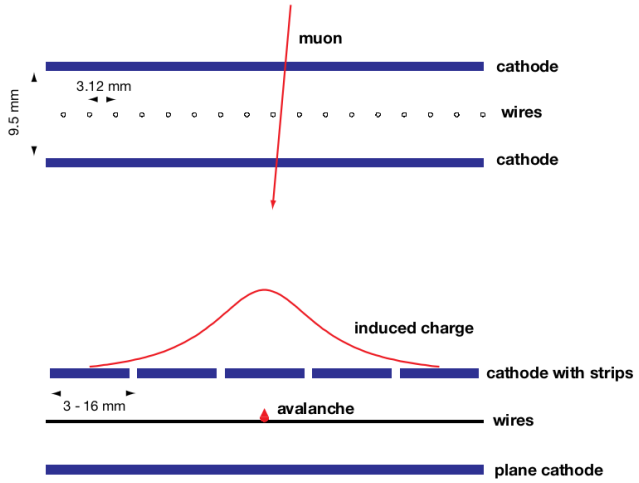

Figure 2-7. A Cathode Strip Chamber **?**

2.2.3.3 Resistive Plate Chambers

The RPCs are located both in the barrel and in the end caps. The RPCs have excellent timing resolution on the order of 1 ns. The RPCs use their excellent timing resolution to determine each particle's bunch crossing of origin. The accurate and rapid timing information helps with the online selection of muons, a huge priority for CMS considering that many interesting collisions produce muons. For this reason the RPCs focus on efficient online selection of muons instead of accurate offline reconstruction **?**.

In this way the RPCs complement the DTs and CSCs. The RPCs consist of two high resistance parallel plates surrounding a volume of gas. The outsides of the plates are painted with graphite paint forming the electrodes. A large voltage differential is kept between the electrodes. When a charged particle crosses the plates it induces an electrical discharge in the plates which remains localized in time and space due to the large resistivity.

2.2.4 Trigger System

Collision events come at a rate of 10 MHz with each event taking up roughly a MB of information. If the detector had to store all of the information from each event this would amount to pushing terabytes of information into a storage system every second, which is remarkably infeasible. To deal with this issue CMS utilizes a trigger system, which selects only

interesting events cutting the rate down from 10 MHz to 1 KHz **?**. Since bunch crossings happen every 25 ns the trigger needs to operate at an incredibly high rate.

CMS tackled this issue by dividing the trigger into different tiers. The Level 1 Trigger is the first stage of the trigger system made from custom hardware which can operate at fantastic speed. The Level 1 Trigger reduces the rate from 10 MHz to 100 KHz and the events passing the L1 Trigger go onto the High Level Trigger (HLT) which further reduces the rate to 1 KHz. Due to the lower input rate the HLT can operate in software.

2.2.4.1 L1 Trigger

The L1 Trigger is made of up different subsystems that work together to decide whether to keep the data from a beam crossing for further processing. The University of Florida works with the Level 1 muon trigger system, the Endcap Muon Track Finder (EMTF) in particular. The muon system needs to determine the transverse momenta of muons and their location and choose the best candidates. Each of the different muon detectors have their own local triggers which send their best muon tracks to the Global Muon Trigger (GMT). The GMT chooses the best muon candidates from that set and passes these on to the Global Trigger (GT). The GT combines the information from the calorimeter triggering system. The GT uses this combined information to check whether the bunch crossing should be sent to the HLT or discarded. The L1 Trigger has many different trigger criteria defining separate triggers which are the trigger bits. If an event passes any of the triggers then it is forwarded for further processing.

The Track Finders (TF) play an important role in the L1 Trigger system. The EMTF combines the location and direction information from the different CSC stations into muon tracks and calculates the transverse momenta for the different tracks. The EMTF chooses the best candidates (highest momentum and highest quality) to send to the GMT. The Drift Tube Track Finder (DTTF) performs a similar process for muons in the DT system. The RPC system calculates the location and direction and forms tracks in the same stage. In the process the RPC trigger system assigns transverse momenta and quality, and like the others chooses the best tracks to send to the GMT.

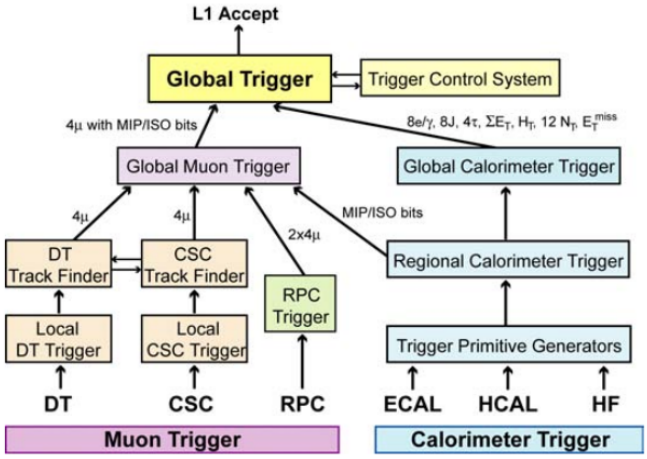

Figure 2-8. The L1 Trigger Architecture **?**

CHAPTER 3
THE STANDARD MODEL

The Standard Model (SM) of particle physics is an incredibly successful theory that correctly describes the physics of all known particles and forces that make up the universe, excluding gravity **?**. The particles of the SM come in two types, fermions and bosons [1] . Fermions are the spin $\frac{1}{2}$ particles and make up the different types of matter. Electrons are a familiar example, and the up and down quarks that make up protons and neutrons are others. While electrons and the up and down quarks account for nearly all of the matter in our day to day experience there are actually many other fermions. In fact, there are three generations of quarks and leptons [2] with each generation heavier than the next. The up and down quarks are the first generation of quarks, charmed and strange are the next, and top and bottom are the third generation. For the leptons the electron and electron neutrino are the first generation, the muon and muon neutrino are the second, and the tau and the tau neutrino the third. Each fermion also has a corresponding antiparticle. As an example, the positron is the antiparticle for the electron.

The universe would be pretty boring if the particles couldn't attract or repel or form more complex objects like atoms, molecules, and even people. Luckily there are forces as well and these forces are described by the spin 1 bosons. The fermions attract and repel by exchanging bosons, which is why the bosons are often called force carriers. Gluons mediate the strong force, photons the electromagnetic force, and the W and Z bosons mediate the weak force. Every force has an associated charge. Just as those particles with electric charge can interact through the electromagnetic force, those with color charge may interact via the strong force, and those with isospin may interact through the weak force. The fundamental forces and particles interact to make the familiar composite objects that surround us in our daily lives.

[1] Bosons have integer spin.

[2] Leptons are fermions that aren't quarks.

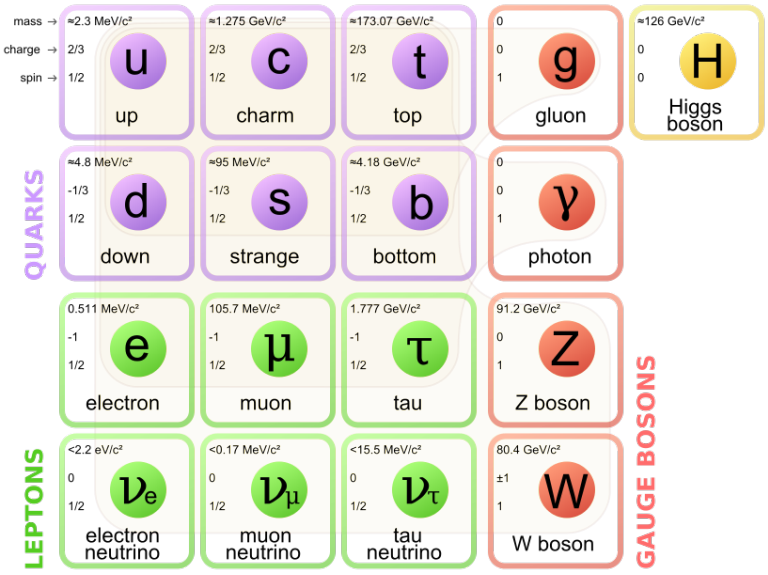

Figure 3-1. The Standard Model Particles

The strong force binds quarks to form protons and neutrons, the Van Der Waals version of the strong force binds the protons and neutrons together to form nuclei, and the electromagnetic force binds electrons and nuclei to form atoms. The size of the composite objects gives an idea of the relative strength of the forces. A proton is $10^{-}15$ meters in size while an atom is $10^{-}10$ meters and a solar system is $10^{1}2$ meters. The more tightly bound the stronger the force. In fact the ratio of the strength of the forces is like so $1{:}10^{-}3{:}10^{-}16{:}10^{-}41$, strong : electromagnetic : weak :gravitational [3] .

Of all the particles predicted by the SM, only the Higgs boson remains to be found. The Higgs boson is the only spin 0 particle of the SM. It is theorized that as the universe cooled from the Big Bang the Higgs field went through a phase transition and settled into a nonzero ground state forming a condensate. And it is the potential energy from the interactions with this nonzero ground state that give the massive fundamental particles their mass. With such a large role in the SM, finding this particle or a BSM Higgs has been a huge priority for the

[3] Gravity is just included for perspective. The Standard Model does not describe this force and reconciling gravity with quantum mechanics is an open problem.

CMS collaboration **?**. In 2012 a Higgs particle with a mass of 125 GeV was found and to date remains consistent with the Standard Model. However, the properties need to be investigated further before declaring the discovered Higgs the Higgs of the Standard Model.

3.1 Quantum Field Theory

The mathematical framework used to describe the physics of the SM as well as other Beyond Standard Model (BSM) field theories is called Quantum Field Theory (QFT). QFT enables the predictions of measurable quantities, namely the probabilities for different sets of particles to come out of a specific collision or for a single particle to decay into different sets of particles. These probabilities are encompassed in the cross sections and branching fractions. For example, the theory of the SM predicts the cross section for two protons colliding and making a Higgs. As another example, the SM also predicts the branching fraction for a Z boson decaying to two muons. These probabilities can be measured simply by colliding particles and counting the outcomes which in turn means that the theory can be tested. In fact, any QFT model can be tested in this manner. There are other commonly measured properties as well like the lifetime, spin, and mass of different particles.

3.1.1 What is a Particle?

Since QFT makes quantitative predictions in terms of particle collisions and particle decays it's interesting to contemplate what a particle really is. The idea of a particle is often taken for granted. Consider an observer in a frame x with particle p and an observer in another frame x'. If the observer in x' can't identify particle p then it doesn't make sense to call p a particle. More concretely, consider a world where in frame x an observer sees a neatly stacked deck of cards, but in x' the observer sees the cards scattered all over the place. Calling the deck of cards a particle doesn't really make sense. On the other hand, both parties can still agree on the individual cards which kept the same suit and value. These are conserved quantities. If the two observers get together later and compare notes they can see what happened to each card upon transforming from x to x' and work out a set of rules. The king of hearts may do one thing and the 10 of clubs another. They can then add the different forces

into play repeat the process and compare again. Figuring this all out determines the laws of physics for the fundamental pieces called particles.

This idea leads to Wigner's view: a particle is an object with conserved quantities that observers can agree on between frames. In our universe these labels are the mass, charge, spin, color, and isospin. And because different observers can agree on these quantities they can compare notes and work out the laws of physics for the different types of particles. All that remains is to work out laws that people in different frames can confirm, and this is where the Lagrangian formalism comes into play.

3.1.2 The Lagrangian Formalism

The Lagrangian formalism is a mathematical device that allows physicists to describe the evolution of a physical system over time, and it's within this formalism that QFT can be built. But before building the full mathematics of QFT, a simple example of the free Newtonian particle is given, and the different symmetries are observed. The Newtonian example serves as a starting point, and eventually the theory of the Standard Model will be developed using the symmetries as a roadmap. The fact that the laws of physics are indistinguishable in different inertial frames along with the requirement that the speed of light remain constant in all frames of reference lay the foundation for QFT.

So let's get into the framework. The goal of physics is to describe how a physical system evolves over time, and this evolution is usually given by some differential equation describing the state the system will take in the next interval of time given the current time. Moving from state to state from one interval of time to the next, the system traces out a path in space and time or some other more abstract space of possible states. So how does one get the appropriate differential equation? As it turns out nature tries to minimize the difference between the energy spent [4] and the energy available to spend and it minimizes the action S. In the equation below, L is the Lagrangian, T is the kinetic energy and U is the potential

[4] Spent here just means used as kinetic energy.

energy.

$$\mathrm{S} = \int \mathrm{L}\mathrm{d}\mathrm{t} = \int \mathrm{T} - \mathrm{U}\mathrm{d}\mathrm{t} \tag{3–1}$$

At an extremum of S, $\delta\mathrm{S} = 0$ since S must go down then through a slope of zero and back up or vice versa. This assumes continuity and must be true for all parameters – all directions. So to get the equations of motion just vary the parameters of L and solve for the values that yield zero change in the action.

$$\delta\mathrm{S} = \int \mathrm{L}(\mathrm{z}_1 + \mathrm{d}\mathrm{z}_1, \mathrm{z}_2 + \mathrm{d}\mathrm{z}_2, ...)\mathrm{d}\mathrm{t} - \int \mathrm{L}(\mathrm{z}_1, \mathrm{z}_2, ...)\mathrm{d}\mathrm{t} \tag{3–2}$$

Following this process yields the Euler-Lagrange (differential) equations, describing how the parameters z evolve over time. The z's may be the position and velocity, or the quantum fields, or the temperature and volume or some other set of parameters that describe the system. The Lagrangian for a Newtonian free particle in one dimension is pretty simple and gets the point across.

$$\mathrm{S} = \frac{1}{2}\int \mathrm{m}\dot{\mathrm{x}}^2\mathrm{d}\mathrm{t} \tag{3–3}$$

If the action is at an extremum, perturbing the path x(t) by adding the infinitesimal ϵ(t) leaves the action unchanged.

$$\mathrm{S}' = \frac{1}{2}\int \mathrm{m}(\dot{\mathrm{x}} + \dot{\epsilon})^2\mathrm{d}\mathrm{t} = \frac{1}{2}\int \mathrm{m}(\dot{\mathrm{x}}^2 + 2\dot{\mathrm{x}}\dot{\epsilon} + \dot{\epsilon}^2)\mathrm{d}\mathrm{t} = \frac{1}{2}\int \mathrm{m}(\dot{\mathrm{x}}^2 + 2\dot{\mathrm{x}}\mathrm{d}\dot{\mathrm{x}})\mathrm{d}\mathrm{t} \tag{3–4}$$

$$\delta\mathrm{S} = \mathrm{S}' - \mathrm{S} = 0 = \frac{1}{2}\int \mathrm{m}(\dot{\mathrm{x}}^2 + 2\dot{\mathrm{x}}\dot{\epsilon})\mathrm{d}\mathrm{t} - \frac{1}{2}\int \mathrm{m}\dot{\mathrm{x}}^2\mathrm{d}\mathrm{t} = \int \mathrm{m}\dot{\mathrm{x}}\dot{\epsilon}\mathrm{d}\mathrm{t} \tag{3–5}$$

Since x(t) is fixed at the boundaries of the integral, ϵ must be zero at t_o and t_f, so integrating by parts yields the following equation.

$$\delta S = 0 = \epsilon(t_f)\dot{x}(t_f) - \epsilon(t_o)\dot{x}(t_o) + \int m\ddot{x}\epsilon dt = 0\dot{x}(t_f) - 0\dot{x}(t_o) + \int m\ddot{x}\epsilon dt = \int m\ddot{x}\epsilon dt \quad (3\text{–}6)$$

And this equation must be zero for any infinitesimal deviation ϵ.

$$\delta S = 0 \rightarrow m\ddot{x} = 0 \quad (3\text{–}7)$$

So a free particle keeps the same velocity over time. Note that a Newtonian boost by constant velocity $v \rightarrow v' = v + u$ [5] leaves the equations of motion consistent. In the unprimed frame the particle has velocity v with 0 acceleration. In the primed frame the particle has velocity v + u with 0 acceleration. Both observers see the particle act as if there are zero forces.

$$S = \frac{1}{2}\int m(v+u)^2 dt = \frac{1}{2}\int m(v')^2 dt \rightarrow \delta S = 0 \rightarrow m\frac{d}{dt}(v+u) = m\frac{d}{dt}(v') = 0 \quad (3\text{–}8)$$

If u is not constant but a function of time u(t) then the equations of motion do not describe the same time evolution.

$$m\frac{d}{dt}(v+u) = m\dot{v} + m\dot{u} = 0 \rightarrow \dot{v} = -\dot{u} \quad (3\text{–}9)$$

In the case where u(t) depends upon time, the difference between the primed and unprimed frames' equations of motion is then δF.

$$\delta F = m\frac{d}{dt}(v+u) - m\frac{dv}{dt} = m\dot{v} + m\dot{u} - m\dot{v} = m\dot{u} \quad (3\text{–}10)$$

In the unprimed frame, the particle identified by the mass moves with constant velocity, $\dot{v} = 0$. The observer in the primed frame looks at the particle with the same mass and sees

[5] Renaming $\dot{x}$ as v.

it change velocity given by the equation $\dot{\mathrm{v}} = -\dot{\mathrm{u}}$. As an example, set v and $\mathrm{u}, \dot{\mathrm{u}}$ to zero for all times before t=0, and let $\mathrm{u}, \dot{\mathrm{u}}$ turn on after time 0. Both observers will agree that the particle is stationary up until time 0. After which, the observer in the primed frame will see the particle accelerate in strange ways. Meanwhile, the unprimed frame will continue to observe a stationary particle.

In general, every inertial frame finds $\delta\mathrm{F} = 0$ and every accelerating frame finds an extra force $\delta\mathrm{F}$ unique to its acceleration. In this way no observer in an inertial frame can perform an experiment and determine which inertial frame he or she is in. On the other hand, each accelerating frame is identified by its $\delta\mathrm{F}$. In every inertial frame a ball released at rest remains at rest. In an accelerating frame the ball will accelerate according to the motion of the frame $\delta\mathrm{F}$ and this change in the laws of physics identifies the frame in a unique way. Conversely, the laws of physics remain the same boosting between inertial frames, and this invariance is a symmetry of physics. Of course this example is Newtonian and the correct way to boost is given by the Lorentz transformation from Special Relativity, but this gets the point across.

Delving further along the path of symmetry, the fundamental forces depend only on the distance from the charge and not the direction implying that rotations are also a symmetry. This can be seen by looking at the Lagrangian.

$$\mathrm{L} = \frac{1}{2}\mathrm{m}\dot{\vec{\mathrm{x}}}^2 - \mathrm{U}((\vec{\mathrm{x}} - \vec{\mathrm{x}'})^2) \tag{3–11}$$

Rotations leave dot products and consequently the magnitude of vectors unchanged so the Lagrangian is invariant under this transformation. Naturally if the Lagrangian is invariant the equations of motion will be as well.

$$\mathrm{m}\frac{\mathrm{d}\vec{\mathrm{v}}}{\mathrm{dt}} = \vec{\nabla}\mathrm{U} \tag{3–12}$$

In the equations of motion above, both sides are vectors and vectors transform the same way under rotations so the equations of motion are invariant. Note that in the case of rotations both the Lagrangian and the equations of motion are invariant. While for Newtonian

boosts only the equations of motion were invariant. This is due to the fact that Newtonian mechanics is the low velocity limit of relativistic mechanics. In the theory of Special Relativity the action for a massive free particle is written like so.

$$\mathrm{S} = \int \frac{\mathrm{m}}{2} \mathrm{u}^{\mu} \mathrm{u}_{\mu} \mathrm{d}\tau \tag{3–13}$$

Just as rotations preserve the dot product, Lorentz transformations (boosts and rotations) preserve the four vector product. Insofar, both the relativistic Lagrangian and the resulting equations of motion remain invariant under a boost or rotation to a new inertial frame. Building the Lagrangian out of four vector products gaurantees this. Interestingly enough, by studying the properties of the Lorentz group it's possible to find even more fundamental building blocks called spinors.

3.1.3 QFT From Symmetry

The laws of physics are invariant under boosts and rotations, and the Lagrangian provides a mathematical framework for physical predictions. These facts together imply that there's a good shot at building a proper QFT by creating the appropriate invariant Lagrangian. Four vector products remain invariant under Lorentz transformations so they are a natural ingredient, but there are other mathematical objects that could be used as well. In this vein, the symmetries under rotations and boosts are investigated in order to look for some other building blocks. The goal is to find two different representations of the Lorentz group and use one representation to describe fermions and other for bosons.

3.1.3.1 Rotations

Rotations in three dimensions are described by the SO(3) group. Rotations preserve the lengths of vectors and the angles between them, which means that dot products between vectors remain invariant as well. In three dimensions one can rotate about any of the three axes. The rotations about the x, y, and z axes may be characterized by the matrices below.

$$\mathrm{R_x} = \begin{pmatrix} 1 & 0 & 0 \\ 0 & \cos\theta_\mathrm{x} & -\sin\theta_\mathrm{x} \\ 0 & \sin\theta_\mathrm{x} & \cos\theta_\mathrm{x} \end{pmatrix} \tag{3–14}$$

$$\mathrm{R_y} = \begin{pmatrix} \cos\theta_\mathrm{y} & 0 & \sin\theta_\mathrm{y} \\ 0 & 1 & 0 \\ -\sin\theta_\mathrm{y} & 0 & \cos\theta_\mathrm{y} \end{pmatrix} \tag{3–15}$$

$$\mathrm{R_z} = \begin{pmatrix} \cos\theta_\mathrm{z} & -\sin\theta_\mathrm{z} & 0 \\ \sin\theta_\mathrm{z} & \cos\theta_\mathrm{z} & 0 \\ 0 & 0 & 1 \end{pmatrix} \tag{3–16}$$

These rotations may be built up from repeated rotations by an infinitesimally small angle $\mathrm{d}\theta$. The matrices characterizing an infinitesimal rotation are given by taking the limit as θ goes to zero.

$$\mathrm{dR_x} = \begin{pmatrix} 1 & 0 & 0 \\ 0 & 1 & -\mathrm{d}\theta_\mathrm{x} \\ 0 & \mathrm{d}\theta_\mathrm{x} & 1 \end{pmatrix} = 1 - \mathrm{i}\mathrm{d}\theta_\mathrm{x} \begin{pmatrix} 0 & 0 & 0 \\ 0 & 0 & -\mathrm{i} \\ 0 & \mathrm{i} & 0 \end{pmatrix} = 1 - \mathrm{i}\mathrm{d}\theta_\mathrm{x}\mathrm{J_x} \tag{3–17}$$

$$\mathrm{dR_y} = \begin{pmatrix} 1 & 0 & \mathrm{d}\theta_\mathrm{y} \\ 0 & 1 & 0 \\ -\mathrm{d}\theta_\mathrm{y} & 0 & 1 \end{pmatrix} = 1 - \mathrm{i}\mathrm{d}\theta_\mathrm{y} \begin{pmatrix} 0 & 0 & \mathrm{i} \\ 0 & 0 & 0 \\ -\mathrm{i} & 0 & 0 \end{pmatrix} = 1 - \mathrm{i}\mathrm{d}\theta_\mathrm{y}\mathrm{J_y} \tag{3–18}$$

$$\mathrm{dR_z} = \begin{pmatrix} 1 & -\mathrm{d}\theta_\mathrm{z} & 0 \\ \mathrm{d}\theta_\mathrm{z} & 1 & 0 \\ 0 & 0 & 1 \end{pmatrix} = 1 - \mathrm{i}\mathrm{d}\theta_\mathrm{z} \begin{pmatrix} 0 & -\mathrm{i} & 0 \\ \mathrm{i} & 0 & 0 \\ 0 & 0 & 0 \end{pmatrix} = 1 - \mathrm{i}\mathrm{d}\theta_\mathrm{z}\mathrm{J_z} \tag{3–19}$$

Repeating an infinitesimal rotation many times rebuilds the finite rotation, so the J matrices generate rotations along their respective axes and they are aptly referred to asthe generators of the group. Some algebra reveals this to be the case.

$$\mathrm{R} = (1 - \mathrm{i}\frac{\theta}{\mathrm{N}}\mathrm{J})^{\mathrm{N}} = 1 + (-\mathrm{i}\mathrm{d}\theta\mathrm{J}) + \frac{1}{2!}(-\mathrm{i}\mathrm{d}\theta\mathrm{J})^2 + \frac{1}{3!}(-\mathrm{i}\mathrm{d}\theta\mathrm{J})^3 + ... = \mathrm{e}^{-\mathrm{i}\theta\mathrm{J}} \tag{3–20}$$

Notice that even powers of J yield J^2 and that odd powers of J return J.

$$= 1 - \mathrm{J}^2 + \mathrm{J}^2(1 + \frac{\mathrm{i}^2}{2!}\mathrm{d}\theta^2 + \frac{\mathrm{i}^4}{4!}\mathrm{d}\theta^4 + ...) - \mathrm{i}\mathrm{J}(\mathrm{d}\theta + \frac{\mathrm{i}^2}{3!}\mathrm{d}\theta^3 + \frac{\mathrm{i}^4}{5!}\mathrm{d}\theta^5 + ...) = (1 - \mathrm{J}^2) + \mathrm{J}^2\cos\theta - \mathrm{i}\mathrm{J}\sin\theta \tag{3–21}$$

Plugging in J_z reveals that this process does in fact rebuild the rotation matrix R_z.

$$\begin{aligned} \mathrm{R}_\mathrm{z} &= (\begin{pmatrix} 1 & 0 & 0 \\ 0 & 1 & 0 \\ 0 & 0 & 1 \end{pmatrix} - \begin{pmatrix} 1 & 0 & 0 \\ 0 & 1 & 0 \\ 0 & 0 & 0 \end{pmatrix}) + \begin{pmatrix} 1 & 0 & 0 \\ 0 & 1 & 0 \\ 0 & 0 & 0 \end{pmatrix}\cos\theta_\mathrm{z} + \begin{pmatrix} 0 & -1 & 0 \\ 1 & 0 & 0 \\ 0 & 0 & 0 \end{pmatrix}\sin\theta_\mathrm{z} \\ &= \begin{pmatrix} \cos\theta_\mathrm{z} & -\sin\theta_\mathrm{z} & 0 \\ \sin\theta_\mathrm{z} & \cos\theta_\mathrm{z} & 0 \\ 0 & 0 & 1 \end{pmatrix} \end{aligned} \tag{3–22}$$

Similarly, the other generators rebuild their respective rotation matrices. The generators of the group are actually more fundamental than the rotation matrices. The multiplication table for the generators describes the algebra of the group, which describes the behavior of rotations at a local level. In fact the rotation matrices are just one of the groups with this local algebra, and a specific group obeying the local algebra is analagous to a specific solution of a differential equation: each solution has a different global behavior yet each obeys the same physics. Moreover the multiplication table can be specified without declaring any particular representation for the generators.

$$\begin{aligned} \mathrm{J_x} * \mathrm{J_y} &= \mathrm{i}\mathrm{J_z} + \mathrm{J_y} * \mathrm{J_x} \\ \mathrm{J_y} * \mathrm{J_z} &= \mathrm{i}\mathrm{J_x} + \mathrm{J_z} * \mathrm{J_y} \\ \mathrm{J_z} * \mathrm{J_x} &= \mathrm{i}\mathrm{J_y} + \mathrm{J_x} * \mathrm{J_z} \end{aligned} \tag{3–23}$$

The multiplication table can be specified in a more compact notation using the commutator [6] , $[\mathrm{a}, \mathrm{b}] = \mathrm{ab} - \mathrm{ba}$, and the antisymmetric tensor ϵ.

$$[\mathrm{J_k}, \mathrm{J_l}] = \mathrm{i}\epsilon_{\mathrm{klm}}\mathrm{J_m} \tag{3–24}$$

Finding 3x3 generators that obey the algebra and then repeatedly applying the infinitesimal transormations builds the SO(3) rotation group. The group acts on 3x1 objects called vectors, and these 3x1 vectors are a suitable candidate for a Newtonian Lagrangian. Finding another representation obeying this algebra will provide a more fundamental ingredient for the Lagrangian and allow the construction of a proper QFT. Similar to the way real numbers are built from the squares of imaginary numbers, vectors are built from spinors.

Looking for the lowest order nontrivial nxn matrices satisfying the algebra gives the 2x2 Pauli matrices. The 1x1 matrices are the trival solution: 1x1 matrices are simply scalar complex numbers, which commute and therefore fail to satisfy the algebra unless all of the J matrices are 0. The objects these operators act on are 1x1 numbers called scalars and remain invariant under rotations and correspond to spin 0. The solution for the 2x2 case, the Pauli matrices are given by

$$\sigma_{\mathrm{x}} = \begin{pmatrix} 0 & 1 \\ 1 & 0 \end{pmatrix}, \sigma_{\mathrm{y}} = \begin{pmatrix} 0 & -\mathrm{i} \\ \mathrm{i} & 0 \end{pmatrix}, \sigma_{\mathrm{y}} = \begin{pmatrix} 1 & 0 \\ 0 & -1 \end{pmatrix} \tag{3–25}$$

[6] The Lie Bracket defines the multiplication for a Lie Algebra and this reduces to the commutator for Lie groups of matrices like SO(3). Notice that using the commutator below returns another member of the group and thus the group is closed under commutation.

However, plugging these into the commutator reveals a factor of two difference.

$$[\sigma_{\mathrm{k}}, \sigma_{\mathrm{l}}] = 2\mathrm{i}\epsilon_{\mathrm{klm}}\sigma_{\mathrm{m}} \tag{3–26}$$

Defining $\mathrm{J_k} = \frac{1}{2}\sigma_{\mathrm{k}}$ fixes this. These matrices act on an array of 2x1 complex numbers called spinors, and this new rotation group is called SU(2). Note that by starting with vectors and analyzing the SO(3) rotation group along with its underlying algebra, new mathematical objects have been discovered. The 1x1 matrices satisfying the rotation algebra make up the spin 0 representation of SU(2), the 2x2 matrices acting on 2x1 objects satisfying the algebra make up the spin $\frac{1}{2}$ representation, and the 3x3 matrices acting on 3x1 objects satisfying the algebra make up the spin 1 representation. The pattern continues on. There are in fact many representations of SU(2). It's now possible to use these representations to build rotationally invariant Lagrangians. While rotationally invariant Lagrangians are important for nonrelativistic theories, the real goal is to break down four vectors in the same way to find the most fundamental ingredients for relativistic Lagrangians.

$$[\mathrm{J_k}, \mathrm{J_l}] = \mathrm{i}\epsilon_{\mathrm{klm}}\mathrm{J_m} \tag{3–27}$$

3.1.3.2 The Lorentz Group

Four vector products are invariant with regards to rotations and boosts. This statement is defined by the mathematical equation below, where the Λ matrices represent the rotation/boost matrices of the Lorentz Group [7] and the η matrix is the Minkowski metric $\begin{pmatrix} 1 & 0 & 0 & 0 \\ 0 & -1 & 0 & 0 \\ 0 & 0 & -1 & 0 \\ 0 & 0 & 0 & -1 \end{pmatrix}$.

$$\mathrm{x}'_{\mu}\mathrm{x}'^{\mu} = \mathrm{x}_{\mu}\mathrm{x}^{\mu} \rightarrow \eta_{\sigma\rho}\Lambda^{\sigma}_{\mu}\Lambda^{\rho}_{\nu}\mathrm{x}^{\mu}\mathrm{x}^{\nu} = \eta_{\mu\nu}\mathrm{x}^{\mu}\mathrm{x}^{\nu} \rightarrow \eta_{\sigma\rho}\Lambda^{\sigma}_{\mu}\Lambda^{\rho}_{\nu} = \eta_{\mu\nu} \tag{3–28}$$

In this 3 + 1 dimensional space the rotations and their corresponding generators are now given by the following R and J matrices.

[7] The Lorentz group dealt with here is the proper orthochronous Lorentz Group SO(1,3).

$$\mathrm{R_x} = \begin{pmatrix} 1 & 0 & 0 & 0 \\ 0 & 1 & 0 & 0 \\ 0 & 0 & \cos\theta_\mathrm{x} & -\sin\theta_\mathrm{x} \\ 0 & 0 & \sin\theta_\mathrm{x} & \cos\theta_\mathrm{x} \end{pmatrix}, \mathrm{J_x} = \begin{pmatrix} 0 & 0 & 0 & 0 \\ 0 & 0 & 0 & 0 \\ 0 & 0 & 0 & -\mathrm{i} \\ 0 & 0 & \mathrm{i} & 0 \end{pmatrix} \tag{3–29}$$

$$\mathrm{R_y} = \begin{pmatrix} 1 & 0 & 0 & 0 \\ 0 & \cos\theta_\mathrm{y} & 0 & \sin\theta_\mathrm{y} \\ 0 & 0 & 1 & 0 \\ 0 & -\sin\theta_\mathrm{y} & 0 & \cos\theta_\mathrm{y} \end{pmatrix}, \mathrm{J_y} = \begin{pmatrix} 0 & 0 & 0 & 0 \\ 0 & 0 & 0 & \mathrm{i} \\ 0 & 0 & 0 & 0 \\ 0 & -\mathrm{i} & 0 & 0 \end{pmatrix} \tag{3–30}$$

$$\mathrm{R_z} = \begin{pmatrix} 1 & 0 & 0 & 0 \\ 0 & \cos\theta_\mathrm{z} & -\sin\theta_\mathrm{z} & 0 \\ 0 & \sin\theta_\mathrm{z} & \cos\theta_\mathrm{z} & 0 \\ 0 & 0 & 0 & 1 \end{pmatrix}, \mathrm{J_z} = \begin{pmatrix} 0 & 0 & 0 & 0 \\ 0 & 0 & -\mathrm{i} & 0 \\ 0 & \mathrm{i} & 0 & 0 \\ 0 & 0 & 0 & 0 \end{pmatrix} \tag{3–31}$$

And the boosts are given by the following B matrices.

$$\mathrm{B_x} = \begin{pmatrix} \cosh\omega_\mathrm{x} & \sinh\omega_\mathrm{x} & 0 & 0 \\ \sinh\omega_\mathrm{x} & \cosh\omega_\mathrm{x} & 0 & 0 \\ 0 & 0 & 1 & 0 \\ 0 & 0 & 0 & 1 \end{pmatrix} \tag{3–32}$$

$$\mathrm{B_y} = \begin{pmatrix} \cosh\omega_\mathrm{y} & 0 & \sinh\omega_\mathrm{y} & 0 \\ 0 & 1 & 0 & 0 \\ \sinh\omega_\mathrm{y} & 0 & \cosh\omega_\mathrm{y} & 0 \\ 0 & 0 & 0 & 1 \end{pmatrix} \tag{3–33}$$

$$\mathrm{B_z} = \begin{pmatrix} \cosh\omega_\mathrm{z} & 0 & 0 & \sinh\omega_\mathrm{z} \\ 0 & 1 & 0 & 0 \\ 0 & 0 & 1 & 0 \\ \sinh\omega_\mathrm{z} & 0 & 0 & \cosh\omega_\mathrm{z} \end{pmatrix} \tag{3–34}$$

Looking at the differential boosts yields the generators K.

$$\mathrm{dB_x} = \begin{pmatrix} 1 & \mathrm{d}\omega_\mathrm{x} & 0 & 0 \\ \mathrm{d}\omega_\mathrm{x} & 1 & 0 & 0 \\ 0 & 0 & 1 & 0 \\ 0 & 0 & 0 & 1 \end{pmatrix} = 1 + \mathrm{d}\omega_\mathrm{x} \begin{pmatrix} 0 & 1 & 0 & 0 \\ 1 & 0 & 0 & 0 \\ 0 & 0 & 0 & 0 \\ 0 & 0 & 0 & 0 \end{pmatrix} = 1 + \mathrm{d}\omega_\mathrm{x}\mathrm{K_x} \tag{3–35}$$

$$\mathrm{dB_y} = \begin{pmatrix} 1 & 0 & \mathrm{d}\omega_\mathrm{y} & 0 \\ 0 & 1 & 0 & 0 \\ \mathrm{d}\omega_\mathrm{y} & 0 & 1 & 0 \\ 0 & 0 & 0 & 1 \end{pmatrix} = 1 + \mathrm{d}\omega_\mathrm{y} \begin{pmatrix} 0 & 0 & 1 & 0 \\ 0 & 0 & 0 & 0 \\ 1 & 0 & 0 & 0 \\ 0 & 0 & 0 & 0 \end{pmatrix} = 1 + \mathrm{d}\omega_\mathrm{y}\mathrm{K_y} \tag{3–36}$$

$$\mathrm{dB_z} = \begin{pmatrix} 1 & 0 & 0 & \mathrm{d}\omega_\mathrm{z} \\ 0 & 1 & 0 & 0 \\ 0 & 0 & 1 & 0 \\ \mathrm{d}\omega_\mathrm{z} & 0 & 0 & 1 \end{pmatrix} = 1 + \mathrm{d}\omega_\mathrm{z} \begin{pmatrix} 0 & 0 & 0 & 1 \\ 0 & 0 & 0 & 0 \\ 0 & 0 & 0 & 0 \\ 1 & 0 & 0 & 0 \end{pmatrix} = 1 + \mathrm{d}\omega_\mathrm{z}\mathrm{K_z} \tag{3–37}$$

As before with the algebra for rotations in three dimensions the Lorentz algebra is defined by its multiplication table, but now there are rotations and boosts. The multiplication table is given by the commutation relations below, which can be confirmed by brute force computation.

$$[\mathrm{J_i}, \mathrm{J_j}] = \mathrm{i}\epsilon_{\mathrm{ijk}}\mathrm{J_k} \tag{3–38}$$

$$[\mathrm{J_i}, \mathrm{K_j}] = \mathrm{i}\epsilon_{\mathrm{ijk}}\mathrm{K_k} \tag{3–39}$$

$$[\mathrm{K_i}, \mathrm{K_j}] = -\mathrm{i}\epsilon_{\mathrm{ijk}}\mathrm{J_k} \tag{3–40}$$

Notice that the commutator between J matrices returns another J matrix, but that the commutator between K matrices returns a J matrix. This means that the J operators form their own subgroup, and the K operators don't. On the other hand, mixing the Js and Ks up by defining the $\mathrm{Y}^{\pm}$ operators allows the Lorentz algebra to be represented by two independent subgroups.

$$\mathrm{Y}^{\pm} = \frac{1}{2}(\mathrm{J_i} \pm \mathrm{iK_i}) \tag{3–41}$$

$$[\mathrm{Y}_{\mathrm{i}}^{\pm}, \mathrm{Y}_{\mathrm{j}}^{\pm}] = \mathrm{i}\epsilon_{\mathrm{ijk}}\mathrm{Y}_{\mathrm{k}}^{\pm} \tag{3–42}$$

$$[\mathrm{Y}_{\mathrm{i}}^{\pm}, \mathrm{Y}_{\mathrm{j}}^{\mp}] = 0 \tag{3–43}$$

Both of the Y groups have the same commutation relations as SU(2). In this way, the Lorentz algebra can be viewed as if two SU(2) rotation algebras have been glued together. This is similar to the way in which orthogonal basis vectors are stuck together to create a larger dimensional space. In order to figure out how to use this space to build the appropriate Lagrangians, the individual spaces will be investigated. Looking along the Y^{+} axis is akin to setting Y^{-} to zero. Using $(\mathrm{y_+}, \mathrm{y_-})$ to label the representation, the simplest nontrivial case along one axis is spin $\frac{1}{2}$ x spin 0, given by $(\frac{1}{2}, 0)$.

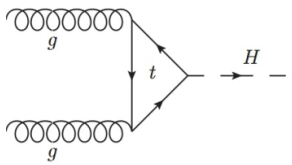

Figure 3-2. The Feynman diagram for two gluons fusing into a Higgs. There are three vertices and this is a third order diagram. Two vertices involve the strong force and one vertex involves the Higgs coupling. The matrix element for this diagram would have two factors of the strong force coupling and one factor for the Higgs coupling which involves the mass of the top quark.

3.1.3.3 Building Lagrangians

3.1.4 Perturbation Theory

3.1.5 Feynman Rules

3.2 The Standard Model Higgs

3.2.1 SM Higgs Production and Decay Modes

The SM Higgs can be created in a variety of ways. Some of these cross sections are shown below for 14 TeV collisions. The production cross sections are functions of the mass of the Higgs as well as the energy of the collisons. For a given collision energy the cross sections decrease as the Higgs mass increases: there are fewer kinematic possibilities for a heavier particle since more of the energy was used to create the particle. For a given mass, say 125 GeV, the cross section grows with collision energy. This constrasts with cross sections involving collisions of fundamental particles, e.g. electron antielectron collisions. This is an artifact of the fact that the LHC collides protons together.

Protons behave like a collection of an infinite number of quark-antiquarks, an infinite number of gluons, and the usual uud. The total momentum of the proton is divided up amongst them with lots of particles having little of the total momentum. The actual scattering events are between these more fundamental particles. The larger the total energy the smaller the fraction of energy needed to make a Higgs and since there are more particles with a lower fraction, this results in a growth of the cross section with collision energy.

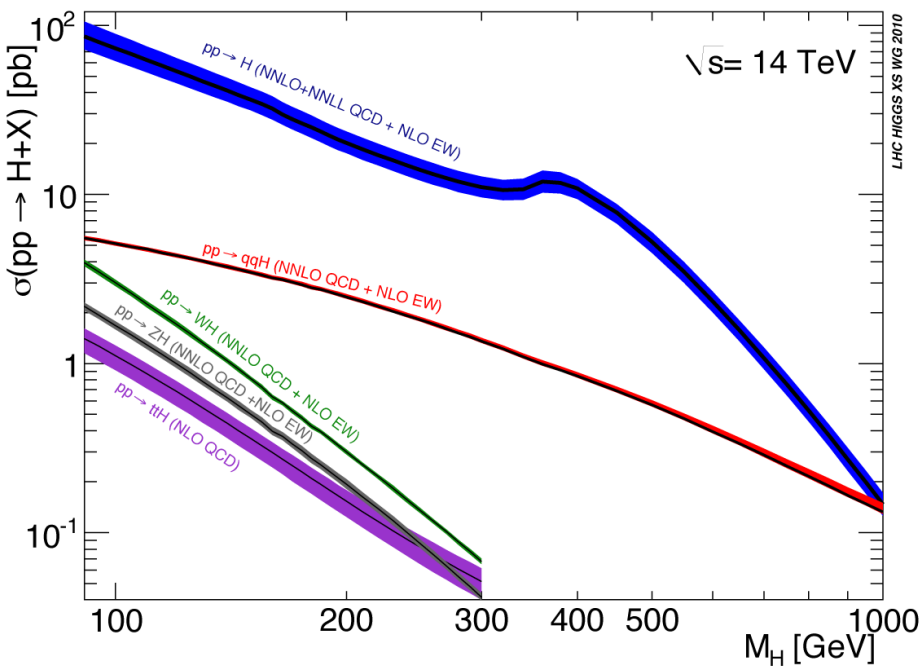

Figure 3-3. The highest production mode cross sections for the SM Higgs **?**

The SM Higgs is unstable and decays with a width of $\sim$ $5\mathrm{MeV}$ at 125 GeV. The probability of each decay changes depending upon the mass of the Higgs. In general the Higgs couples more strongly to particles with higher mass making the decays to heavier particles more likely.

The muon has the lowest mass – excluding the photon and gluon – of the particles in Figure 3-4 and consequently H$\rightarrow \mu^+\mu^-$ has the lowest branching fraction in the set. [8] The gluons and photons are massless and do not couple to the Higgs at leading order. These massless vector bosons interact with the Higgs through a loop of top quarks. The extremely heavy mass of the top quark, about 173 GeV, balances the fact that the loop production is a higher order mechanism.

[8] The Higgs also couples to the electron and the first generation quarks but the masses are so light that CMS does not expect to see the SM Higgs in those modes.

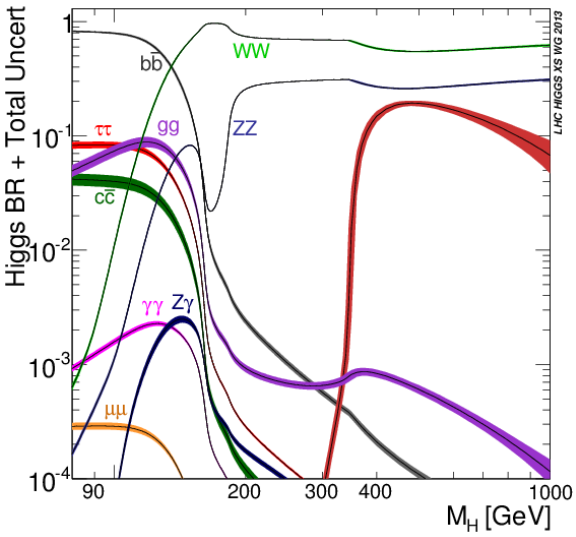

Higgs Branching Ratios	
$b\bar{b}$	0.57
WW	0.22
gg	0.085
$\tau\tau$	0.065
ZZ	0.027
$c\bar{c}$	0.027
$\gamma\gamma$	0.0023
$Z\gamma$	0.0016
$\mu^+\mu^-$	0.00022

Figure 3-4. The graphic on the top left presents the SM Higgs branching fractions as functions of mass while the table on the bottom right displays the branching fractions for a 125 GeV SM Higgs **?**.

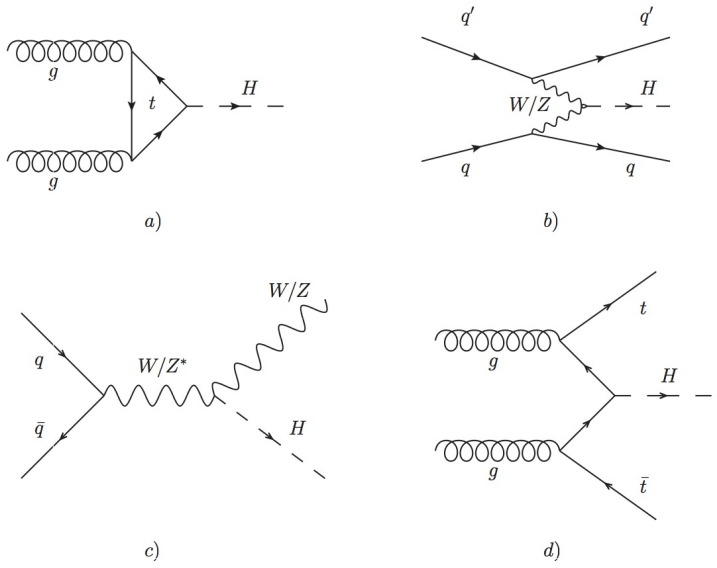

Figure 3-5. The SM production modes with the highest cross sections. a) Gluon Gluon Fusion (GF) b) Vector Boson Fusion (VBF) c) Associated Production with a Vector Boson (VH) d) $t\bar{t}H$

The Higgs to massless vector boson coupling via the top loop is seen in the GF Feynman diagram in Figure 3-5. At $M_h = 125$ GeV, $\sqrt{s} = 13$ TeV, the GF channel comprises 87% of the total Higgs production cross section, VBF 7%, VH 4%, and $t\bar{t}H$ 1% **?**. Besides $t\bar{t}H$, the process $q + \bar{q} \rightarrow H$ isn't considered due to its low cross section. The low masses of the other quarks suppress the process.

Quark gluon (qg) scattering is a major background for the Higgs to two jets decays since the process closely resembles GF in this mode.

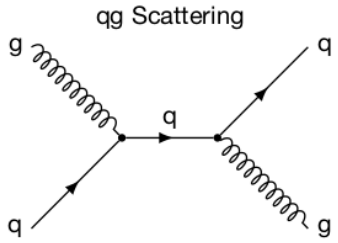

Figure 3-6. Quark gluon scattering creates many two jet events. This background looks very similar to GF when the Higgs decays to two jets. The colliding protons are made of quarks and gluons so this process is extremely common.

CHAPTER 4
RESULTS

4.1 Fusce Eget Tempus Lectus,

Algorithm 4.1. *Euclids algorithm*

```
1: procedure EUCLID(a, b)                          ▷ The g.c.d. of a and b
2:     r ← a mod b
3:     while r ≠ 0 do                              ▷ We have the answer if r is 0
4:         a ← b
5:         b ← r
6:         r ← a mod b
7:     end while
8:     return b                                    ▷ The gcd is b
9: end procedure
```

Proposition 4.1. *The Upsilon Function*

(1) If $\beta > 0$ *and* $\alpha \neq 0$*, then for all* $\mathrm{n} \geq -1$*,*

$$\mathrm{I_n}(\mathrm{c};\alpha;\beta;\delta) = -\frac{\mathrm{e}^{\alpha \mathrm{c}}}{\alpha}\sum_{\mathrm{i}=0}^{\mathrm{n}}(\frac{\beta}{\alpha})^{\mathrm{n}-\mathrm{i}}\mathrm{Hh_i}(\beta \mathrm{c}-\delta)$$

$$+(\frac{\beta}{\alpha})^{\mathrm{n}+1}\frac{\sqrt{2\pi}}{\beta}\mathrm{e}^{\frac{\alpha\delta}{\beta}+\frac{\alpha^2}{2\beta^2}}\phi(-\beta \mathrm{c}+\delta+\frac{\alpha}{\beta})$$

(2) If $\beta < 0$ *and* $\alpha < 0$*, then for all* $\mathrm{x} \geq -1$

$$\mathrm{I_n}(\mathrm{c};\alpha;\beta;\delta) = -\frac{\mathrm{e}^{\alpha \mathrm{c}}}{\alpha}\sum_{\mathrm{i}=0}^{\mathrm{n}}(\frac{\beta}{\alpha})^{\mathrm{n}-\mathrm{i}}\mathrm{Hh_i}(\beta \mathrm{c}-\delta)$$

$$-(\frac{\beta}{\alpha})^{\mathrm{n}+1}\frac{\sqrt{2\pi}}{\beta}\mathrm{e}^{\frac{\alpha\delta}{\beta}+\frac{\alpha^2}{2\beta^2}}\phi(\beta \mathrm{c}-\delta-\frac{\alpha}{\beta})$$

Proof. Case 1.

$\beta > 0$ and $\alpha \neq 0$. Since, for any constant α and $\mathrm{n} \geq 0$, $\mathrm{e}^{\alpha \mathrm{x}}\mathrm{Hh_n}(\beta \mathrm{x}-\delta) \to 0$ as $\mathrm{x} \to \infty$ thanks to (B4), integration by parts leads to

$$\mathrm{I_n} = -\frac{1}{\alpha}\mathrm{Hh}(\beta \mathrm{c}-\delta)\mathrm{e}^{\alpha \mathrm{c}}+\frac{\beta}{\alpha}\int_{\mathrm{c}}^{\infty}\mathrm{e}^{\alpha \mathrm{x}}\mathrm{Hh_{n-1}}(\beta \mathrm{c}-\delta)\mathrm{dx}$$

In other words, we have a recursion, for $\mathrm{n} \geq 0$, $\mathrm{I_n} = -(\mathrm{e}^{\alpha \mathrm{c}}\alpha)\mathrm{Hh_n}(\beta \mathrm{c} - \delta) + (\frac{\beta}{\alpha})\mathrm{I_{n-1}}$ with

$$\mathrm{I_{-1}} = \sqrt{2\pi}\int_{\mathrm{c}}^{\infty} \mathrm{e}^{\alpha \mathrm{x}}\varphi(-\beta \mathrm{x} + \delta)\mathrm{dx}$$

$$= \frac{\sqrt{2\pi}}{\beta}\mathrm{e}^{\frac{\alpha\delta}{\beta} + \frac{\alpha^2}{2\beta^2}}\phi(-\beta \mathrm{c} + \delta + \frac{\alpha}{\beta})$$

Solving it yields, for $\mathrm{n} \geq -1$,

$$\mathrm{I_n} = -\frac{\mathrm{e}^{\alpha \mathrm{c}}}{\alpha}\sum_{\mathrm{i}=0}^{\mathrm{n}}(\frac{\beta}{\alpha})^{\mathrm{i}}\mathrm{Hh_{n-i}}(\beta \mathrm{c} + \delta) + (\frac{\beta}{\alpha})^{\mathrm{n}+1}\mathrm{I_{-1}}$$

$$= -\frac{\mathrm{e}^{\alpha \mathrm{c}}}{\alpha}\sum_{\mathrm{i}=0}^{\mathrm{n}}(\frac{\beta}{\alpha})^{\mathrm{n}-\mathrm{i}}\mathrm{Hh_i}(\beta \mathrm{c} + \delta)$$

$$+(\frac{\beta}{\alpha})^{\mathrm{n}+1}\frac{\sqrt{2\pi}}{\beta}\mathrm{e}^{\frac{\alpha\delta}{\beta} + \frac{\alpha^2}{2\beta^2}}\phi(-\beta \mathrm{c} + \delta + \frac{\alpha}{\beta})$$

where the sum over an empty set is defined to be zero. □

Proof. Case2. $\beta < 0$ and $\alpha < 0$. In this case, we must also have, for $\mathrm{n} \geq 0$ and any constant $\alpha < 0, \mathrm{e}^{\alpha \mathrm{x}}\mathrm{Hh_n}(\beta \mathrm{x} - \delta) \to 0$ as

$\mathrm{x} \to \infty$, thanks to (B5). Using integration by parts, we again have the same recursion, for $\mathrm{n} \geq 0, \mathrm{I_n} = -(\mathrm{e}^{\alpha \mathrm{c}}/\alpha)\mathrm{Hh_n}(\beta \mathrm{c} - \delta) + (\beta/\alpha)\mathrm{I_{n-1}}$, but with a different initial condition

$$\mathrm{I_{-1}} = \sqrt{2\pi}\int_{\mathrm{c}}^{\infty} \mathrm{e}^{\alpha \mathrm{x}}\varphi(-\beta \mathrm{x} + \delta)\mathrm{dx}$$

$$= -\frac{\sqrt{2\pi}}{\beta}\exp\{\frac{\alpha\delta}{\beta} + \frac{\alpha^2}{2\beta^2}\}\phi(\beta \mathrm{c} - \delta - \frac{\alpha}{\beta})$$

Solving it yields (B8), for $\mathrm{n} \geq -1$.

□

Finally, we sum the double exponential and the normal random variables

Proposition B.3.

Suppose $\{\xi_1, \xi_2, ...\}$ *is a sequence of i.i.d. exponential random variables with rate* $\eta > 0$, *and Z is a normal variable with distribution* $\mathrm{N}(0, \sigma^2)$. *Then for every* $\mathrm{n} \geq 1$, *we have: (1) The density functions are given by:*

$$\mathrm{f}_{\mathrm{Z}+\sum_{\mathrm{i}=1}^{\mathrm{n}} \xi_{\mathrm{i}}}(\mathrm{t}) = (\sigma\eta)^{\mathrm{n}} \frac{\mathrm{e}^{(\sigma\eta)^2/2}}{\sigma\sqrt{2\pi}} \mathrm{e}^{-\mathrm{t}\eta} \mathrm{Hh}_{\mathrm{n}-1}(-\frac{\mathrm{t}}{\sigma} + \sigma\eta)$$

$$\mathrm{f}_{\mathrm{Z}-\sum_{\mathrm{i}=1}^{\mathrm{n}} \xi_{\mathrm{i}}}(\mathrm{t}) = (\sigma\eta)^{\mathrm{n}} \frac{\mathrm{e}^{(\sigma\eta)^2/2}}{\sigma\sqrt{2\pi}} \mathrm{e}^{-\mathrm{t}\eta} \mathrm{Hh}_{\mathrm{n}-1}(\frac{\mathrm{t}}{\sigma} + \sigma\eta)$$

(2) The tail probabilities are given by

$$\mathrm{P}(\mathrm{Z} + \sum_{\mathrm{i}=1}^{\mathrm{n}} \xi_{\mathrm{i}} \geq \mathrm{x}) = (\sigma\eta)^{\mathrm{n}} \frac{\mathrm{e}^{(\sigma\eta)^2/2}}{\sigma\sqrt{2\pi}} \mathrm{e}^{-\mathrm{t}\eta} \mathrm{I}_{\mathrm{n}-1}(\mathrm{x}; -\eta, -\frac{1}{\sigma}, -\sigma\eta)$$

$$\mathrm{P}(\mathrm{Z} - \sum_{\mathrm{i}=1}^{\mathrm{n}} \xi_{\mathrm{i}} \geq \mathrm{x}) = (\sigma\eta)^{\mathrm{n}} \frac{\mathrm{e}^{(\sigma\eta)^2/2}}{\sigma\sqrt{2\pi}} \mathrm{e}^{-\mathrm{t}\eta} \mathrm{I}_{\mathrm{n}-1}(\mathrm{x}; \eta, \frac{1}{\sigma}, -\sigma\eta)$$

Proof. Case 1. The densities of $\mathrm{Z} + \sum_{\mathrm{i}=1}^{\mathrm{n}} \xi_{\mathrm{i}}$, *and* $\mathrm{Z} - \sum_{\mathrm{i}=1}^{\mathrm{n}} \xi_{\mathrm{i}}$. *We have*

$$\mathrm{f}_{\mathrm{Z}+\sum_{\mathrm{i}=1}^{\mathrm{n}} \xi_{\mathrm{i}}}(\mathrm{t}) = \int_{-\infty}^{\infty} \mathrm{f}_{\sum_{\mathrm{i}=1}^{\mathrm{n}} \xi_{\mathrm{i}}}(\mathrm{t} - \mathrm{x}) \mathrm{f}_{\mathrm{Z}}(\mathrm{x}) \mathrm{dx}$$

$$= \mathrm{e}^{-\mathrm{t}\eta}(\eta^{\mathrm{n}}) \int_{-\infty}^{\mathrm{t}} \frac{\mathrm{e}^{\mathrm{x}\eta}(\mathrm{t} - \mathrm{x})^{\mathrm{n}-1}}{(\mathrm{n}-1)!} \frac{1}{\sigma\sqrt{2\pi}} \mathrm{e}^{-\mathrm{x}^2/(2\sigma^2)} \mathrm{dx}$$

$$= \mathrm{e}^{-\mathrm{t}\eta}(\eta^{\mathrm{n}}) \mathrm{e}^{(\sigma\eta)^2/(2)} \int_{-\infty}^{\mathrm{t}} \frac{(\mathrm{t} - \mathrm{x})^{\mathrm{n}-1}}{(\mathrm{n}-1)!} \frac{1}{\sigma\sqrt{2\pi}} \mathrm{e}^{-(\mathrm{x}-\sigma^2\eta)^2/(2\sigma^2)} \mathrm{dx}$$

Letting $\mathrm{y} = (\mathrm{x} - \sigma^2\eta)/\sigma$ *yields*

$$\mathrm{f}_{\mathrm{Z}+\sum_{\mathrm{i}=1}^{\mathrm{n}} \xi_{\mathrm{i}}}(\mathrm{t}) = \mathrm{e}^{-\mathrm{t}\eta}(\eta^{\mathrm{n}}) \mathrm{e}^{(\sigma\eta)^2/(2)} \sigma^{\mathrm{n}-1}$$

$$\times \int_{-\infty}^{\mathrm{t}/\sigma - \sigma\eta} \frac{(\mathrm{t}/\sigma - \mathrm{y} - \sigma\eta)^{\mathrm{n}-1}}{(\mathrm{n}-1)!} \frac{1}{\sqrt{2\pi}} \mathrm{e}^{-\mathrm{y}^2/2} \mathrm{dy}$$

$$= \frac{e^{(\sigma\eta)^2/2}}{\sqrt{2\pi}}(\sigma^{n-1}\eta^n)e^{-t\eta}Hh_{n-1}(-t/\sigma + \sigma\eta)$$

because $(1/(n-1)!)\int_{-\infty} a(a-y)^{n-1}e^{-y^2/2}dy = Hh_{n-1}(a)$. *The derivation of* $f_{Z+\sum_{i=1}^n \xi_i}(t)$ *is similar.*

Case 2. $P(Z + \sum_{i=1}^n \xi_i \geq x)$ *and* $P(Z - \sum_{i=1}^n \xi_i \geq x)$. *From (B9), it is clear that*

$$P(Z + \sum_{i=1}^n \xi_i \geq x) = \frac{(\sigma\eta)^n e^{(\sigma\eta)^2/2}}{\sigma\sqrt{2\pi}} \int_x^\infty e^{(-i\eta)} Hh_{n-1}(-\frac{t}{\sigma} + \sigma\eta)dt$$

$$= \frac{(\sigma\eta)^n e^{(\sigma\eta)^2/2}}{\sigma\sqrt{2\pi}} I_{n-1}(x; -\eta, -\frac{1}{\sigma}, -\sigma\eta)dt$$

by (B6). We can compute $P(Z - \sum_{i=1}^n \xi_i \geq x)$ *similarly.*

Theorem 4.1. *Theorem With* $\pi_n := P(N(t) = n) = e^{-\lambda T}(\lambda T)^n/n!$ *and* I_n *in Proposition* **??**. *, we have*

$$P(Z(T) \geq a) = \frac{e^{(\sigma\eta_1)^2 T/2}}{\sigma\sqrt{2\pi T}} \sum_{n=1}^\infty \pi_n \sum_{k=1}^n P_{n,k}(\sigma\sqrt{T}\eta_1)^k \times I_{k-1}(a - \mu T; -\eta_1, -\frac{1}{\sigma\sqrt{T}}, -\sigma\eta_1\sqrt{T})$$

$$+\frac{e^{(\sigma\eta_2)^2 T/2}}{\sigma\sqrt{2\pi T}} \sum_{n=1}^\infty \pi_n \sum_{k=1}^n Q_{n,k}(\sigma\sqrt{T}\eta_2)^k$$

$$\times I_{k-1}(a - \mu T; \eta_2, \frac{1}{\sigma\sqrt{T}}, -\sigma\eta_2\sqrt{T})$$

$$+\pi_0\phi(-\frac{a - \mu T}{\sigma\sqrt{T}})$$

Proof by the decomposition (B2)

$$P(Z(T) \geq a) = \sum_{n=0}^\infty \pi_n P(\mu T + \sigma\sqrt{T}Z + \sum_{j=1}^n Y_j \geq a)$$

$$= \pi_0 \mathrm{P}(\mu \mathrm{T} + \sigma\sqrt{\mathrm{T}}\mathrm{Z} \geq \mathrm{a})$$

$$+ \sum_{\mathrm{n}=1}^{\infty} \pi_{\mathrm{n}} \sum_{\mathrm{k}=1}^{\mathrm{n}} \mathrm{P}_{\mathrm{n,k}} \mathrm{P}(\mu \mathrm{T} + \sigma\sqrt{\mathrm{T}}\mathrm{Z} + \sum_{\mathrm{j}=1}^{\mathrm{n}} \xi_{\mathrm{j}}^{+} \geq \mathrm{a})$$

$$+ \sum_{\mathrm{n}=1}^{\infty} \pi_{\mathrm{n}} \sum_{\mathrm{k}=1}^{\mathrm{n}} \mathrm{Q}_{\mathrm{n,k}} \mathrm{P}(\mu \mathrm{T} + \sigma\sqrt{\mathrm{T}}\mathrm{Z} - \sum_{\mathrm{j}=1}^{\mathrm{n}} \xi_{\mathrm{j}}^{-} \geq \mathrm{a})$$

The result now follows via (B11) and (B12) for $\eta_1 > 1$ *and* $\eta_2 > 0$.

CHAPTER 5
SUMMARY AND CONCLUSIONS

5.1 Non Porttitor Tellus

Aliquam molestie sed urna quis convallis. Aenean nibh eros, aliquam non eros in, tempus lacinia justo. In magna sapien, blandit a faucibus ac, scelerisque nec purus. Praesent fermentum felis nec massa interdum, vel dapibus mi luctus. Cras id fringilla mauris. Ut molestie eros mi, ut hendrerit nulla tempor et. Pellentesque tortor quam, mattis a scelerisque nec, euismod et odio. Mauris rhoncus metus sit amet risus mattis, eu mattis sem interdum.

5.1.1 Nam Arcu Magna

Semper vel lorem eu, venenatis ultrices est. Nam aliquet ut erat ac scelerisque. Maecenas ut molestie mi. Phasellus ipsum magna, sollicitudin eu ipsum quis, imperdiet cursus turpis. Etiam pretium enim a fermentum accumsan. Morbi vel vehicula enim.

5.1.1.1 Ut pellentesque velit sede

Placerat cursus. Integer congue urna non massa dictum, a pellentesque arcu accumsan. Nulla posuere, elit accumsan eleifend elementum, ipsum massa tristique metus, in ornare neque nisl sed odio. Nullam eget elementum nisi. Duis a consectetur erat, sit amet malesuada sapien. Aliquam nec sapien et leo sagittis porttitor at ut lacus. Vivamus vulputate elit vitae libero condimentum dictum. Nulla facilisi. Quisque non nibh et massa ullamcorper iaculis.

APPENDIX A
THIS IS THE FIRST APPENDIX

Lorem ipsum dolor sit amet, consectetuer adipiscing elit. Maecenas eget magna. Aenean et lorem. Ut dignissim neque at nisi. In hac habitasse platea dictumst. In porta ornare eros. Nunc eu ante. In non est vehicula tellus cursus suscipit. Proin sed libero. Sed risus enim, eleifend in, pellentesque ac, nonummy quis, nulla. Phasellus imperdiet libero nec massa. Ut sapien libero, adipiscing eu, volutpat porttitor, ultricies eget, nisi. Sed odio. Suspendisse potenti. Duis dolor augue, viverra id, porta in, dignissim id, nisl. Vivamus blandit cursus eros. Maecenas sit amet urna sit amet orci nonummy pharetra.

Praesent cursus nibh et mauris. In aliquam felis sit amet ligula. Nulla faucibus nisl eget nisl. Aliquam tincidunt. Mauris eget elit sed massa luctus posuere. Pellentesque suscipit. In odio urna, semper ut, convallis ut, porta et, nibh. Nulla sodales metus nec velit posuere gravida. Cras tristique. Etiam urna risus, accumsan ut, placerat sed, iaculis id, est.

Nullam mi. Pellentesque habitant morbi tristique senectus et netus et malesuada fames ac turpis egestas. Duis vitae metus in massa hendrerit rhoncus. Fusce tortor justo, laoreet eu, facilisis at, gravida et, felis. Donec imperdiet mollis erat. Integer tempus nulla ac lorem. Fusce porttitor. Aenean quis arcu. Morbi consectetuer, leo eu mollis elementum, urna massa malesuada risus, euismod tempor lorem elit ut mauris. Cras elit orci, facilisis ac, mattis iaculis, cursus ac, augue. Donec eget nisl. Pellentesque fermentum sodales nibh. Vivamus non risus. Donec est libero, tincidunt sit amet, pretium vitae, blandit sed, tellus. Nunc diam risus, interdum sed, laoreet quis, varius ac, turpis. In et purus eget nibh vehicula rhoncus. Aenean et neque. Praesent nisl nisi, tempus quis, nonummy ac, auctor a, neque. Suspendisse et metus. Suspendisse non metus eu mauris auctor sagittis.

APPENDIX B
AN EXAMPLE OF A HALF TITLE PAGE

Figure B-1. LaTeX2ϵ. logo

This is how a section should look if the first page is a landscape page. Lorem ipsum dolor sit amet, consectetuer adipiscing elit. Ut sit amet nulla. Integer mauris turpis, dapibus ac, auctor non, vehicula sit amet, magna. Suspendisse eu tellus. Etiam porta. Donec magna. Donec ut dui. In hac habitasse platea dictumst. Nullam suscipit, mi at adipiscing commodo, lorem erat scelerisque erat, non pulvinar leo mi eu metus. Phasellus id felis. Sed quam purus, molestie quis, ultrices nec, dictum at, magna. Proin viverra viverra ante.

Maecenas sagittis magna quis ligula. Duis vestibulum mi a felis. Aenean accumsan mattis massa. Nullam lacus sem, consectetuer non, condimentum sit amet, pharetra ac, odio. Morbi nisi magna, tincidunt sed, placerat nec, tincidunt id, lectus. Donec ac dui non mauris vulputate aliquam. Nullam scelerisque congue pede. Integer ipsum. Vestibulum auctor. Suspendisse eget leo id libero cursus dictum. Sed malesuada. Aliquam imperdiet. Donec dui metus, porta eu, aliquet vel, vulputate vitae, lacus.

Nulla quis purus id turpis luctus feugiat. Fusce feugiat. Proin felis. Morbi elit est, fermentum in, tincidunt vitae, convallis vel, orci. Vestibulum justo. Suspendisse non nisl. Pellentesque pretium adipiscing elit. Phasellus fermentum consequat augue. Sed pede nisl, fermentum vel, vulputate id, sollicitudin sed, ligula. Cras suscipit, quam et euismod sagittis, nisl felis gravida felis, quis pulvinar purus est vel pede. Suspendisse mattis est ac nunc. Curabitur rutrum, turpis sit amet commodo tempus, metus lorem commodo lectus, eget fringilla justo nisi et purus. Ut quam sapien, vehicula quis, rhoncus non, sagittis nec, risus.

Donec eget augue ac lacus adipiscing porta. Maecenas pede. Vivamus molestie. Duis condimentum ligula auctor pede. Nullam ullamcorper rhoncus erat. Ut ornare interdum urna. Suspendisse potenti. Curabitur mattis mauris nec risus. Aenean iaculis turpis eu tortor. Donec nec ante non mauris pellentesque fringilla.

Phasellus vitae dui id orci sodales cursus. Curabitur sed nulla quis mauris tincidunt iaculis. Vivamus semper semper orci. Phasellus suscipit ante vitae leo. Sed arcu ipsum, condimentum id, luctus in, sodales eu, magna. In dictum, arcu quis pharetra vestibulum, ante enim placerat lacus, vitae placerat est leo vitae elit. Pellentesque bibendum enim vulputate eros. Nunc

laoreet. Pellentesque habitant morbi tristique senectus et netus et malesuada fames ac turpis egestas. Praesent purus odio, euismod sit amet, aliquam a, volutpat in, augue. Phasellus id massa. Suspendisse suscipit ligula pharetra dolor. Pellentesque vel pede.

Aliquam pharetra est sit amet magna. Aliquam varius. Donec eu lectus et nisl iaculis porttitor. Morbi mattis, mauris sed luctus hendrerit, nulla velit molestie dolor, ac volutpat urna augue vel quam. Maecenas pellentesque libero et massa. Integer vestibulum, lacus at mattis euismod, nisl arcu commodo lectus, ut euismod dolor ligula sit amet libero. Nam in ligula sit amet ante eleifend aliquet. Phasellus feugiat erat at nulla. Proin in lectus. Proin laoreet leo laoreet leo congue lacinia. Quisque non diam sit amet enim ultrices commodo. Praesent fermentum lectus sed ligula. Integer pulvinar accumsan pede. Quisque molestie ligula eget odio. Vestibulum ante ipsum primis in faucibus orci luctus et ultrices posuere cubilia Curae;

APPENDIX C
DERIVATION OF THE Υ FUNCTION

Proposition C.1. *The Upsilon Function*

(1) If $\beta > 0$ *and* $\alpha \neq 0$*, then for all* $\mathrm{n} \geq -1$*,*

$$\mathrm{I_n}(\mathrm{c};\alpha;\beta;\delta) = -\frac{\mathrm{e}^{\alpha \mathrm{c}}}{\alpha}\sum_{\mathrm{i}=0}^{\mathrm{n}}(\frac{\beta}{\alpha})^{\mathrm{n}-\mathrm{i}}\mathrm{Hh_i}(\beta \mathrm{c}-\delta)$$

$$+(\frac{\beta}{\alpha})^{\mathrm{n}+1}\frac{\sqrt{2\pi}}{\beta}\mathrm{e}^{\frac{\alpha\delta}{\beta}+\frac{\alpha^2}{2\beta^2}}\phi(-\beta \mathrm{c}+\delta+\frac{\alpha}{\beta})$$

(2) If $\beta < 0$ *and* $\alpha < 0$*, then for all* $\mathrm{x} \geq -1$

$$\mathrm{I_n}(\mathrm{c};\alpha;\beta;\delta) = -\frac{\mathrm{e}^{\alpha \mathrm{c}}}{\alpha}\sum_{\mathrm{i}=0}^{\mathrm{n}}(\frac{\beta}{\alpha})^{\mathrm{n}-\mathrm{i}}\mathrm{Hh_i}(\beta \mathrm{c}-\delta)$$

$$-(\frac{\beta}{\alpha})^{\mathrm{n}+1}\frac{\sqrt{2\pi}}{\beta}\mathrm{e}^{\frac{\alpha\delta}{\beta}+\frac{\alpha^2}{2\beta^2}}\phi(\beta \mathrm{c}-\delta-\frac{\alpha}{\beta})$$

Proof. Case 1.

$\beta > 0$ and $\alpha \neq 0$. Since, for any constant α and $\mathrm{n} \geq 0$, $\mathrm{e}^{\alpha \mathrm{x}}\mathrm{Hh_n}(\beta \mathrm{x}-\delta) \to 0$ as $\mathrm{x} \to \infty$ thanks to (B4), integration by parts leads to

$$\mathrm{I_n} = -\frac{1}{\alpha}\mathrm{Hh}(\beta \mathrm{c}-\delta)\mathrm{e}^{\alpha \mathrm{c}} + \frac{\beta}{\alpha}\int_{\mathrm{c}}^{\infty}\mathrm{e}^{\alpha \mathrm{x}}\mathrm{Hh_{n-1}}(\beta \mathrm{c}-\delta)\mathrm{dx}$$

In other words, we have a recursion, for $\mathrm{n} \geq 0$, $\mathrm{I_n} = -(\mathrm{e}^{\alpha \mathrm{c}}\alpha)\mathrm{Hh_n}(\beta \mathrm{c}-\delta) + (\frac{\beta}{\alpha})\mathrm{I_{n-1}}$ with

$$\mathrm{I_{-1}} = \sqrt{2\pi}\int_{\mathrm{c}}\infty \mathrm{e}^{\alpha \mathrm{x}}\varphi(-\beta \mathrm{x}+\delta)\mathrm{dx}$$

$$= \frac{\sqrt{2\pi}}{\beta}\mathrm{e}^{\frac{\alpha\delta}{\beta}+\frac{\alpha^2}{2\beta^2}}\phi(-\beta \mathrm{c}+\delta+\frac{\alpha}{\beta})$$

Solving it yields, for $\mathrm{n} \geq -1$,

$$\mathrm{I_n} = -\frac{\mathrm{e}^{\alpha \mathrm{c}}}{\alpha} \sum_{\mathrm{i}=0}^{\mathrm{n}} (\frac{\beta}{\alpha})^{\mathrm{i}} \mathrm{Hh_{n-i}}(\beta \mathrm{c} + \delta) + (\frac{\beta}{\alpha})^{\mathrm{n}+1} \mathrm{I_{-1}}$$

$$= -\frac{\mathrm{e}^{\alpha \mathrm{c}}}{\alpha} \sum_{\mathrm{i}=0}^{\mathrm{n}} (\frac{\beta}{\alpha})^{\mathrm{n}-\mathrm{i}} \mathrm{Hh_i}(\beta \mathrm{c} + \delta)$$

$$+ (\frac{\beta}{\alpha})^{\mathrm{n}+1} \frac{\sqrt{2\pi}}{\beta} \mathrm{e}^{\frac{\alpha\delta}{\beta} + \frac{\alpha^2}{2\beta^2}} \phi(-\beta \mathrm{c} + \delta + \frac{\alpha}{\beta})$$

where the sum over an empty set is defined to be zero. □

Case2. $\beta < 0$ *and* $\alpha < 0$. *In this case, we must also have, for* $\mathrm{n} \geq 0$ *and any constant* $\alpha < 0, \mathrm{e}^{\alpha \mathrm{x}} \mathrm{Hh_n}(\beta \mathrm{x} - \delta) \to 0$ *as*

$\mathrm{x} \to \infty$, *thanks to (B5). Using integration by parts, we again have the same recursion, for* $\mathrm{n} \geq 0, \mathrm{I_n} = -(\mathrm{e}^{\alpha \mathrm{c}}/\alpha) \mathrm{Hh_n}(\beta \mathrm{c} - \delta) + (\beta/\alpha) \mathrm{I_{n-1}}$, *but with a different initial condition*

$$\mathrm{I_{-1}} = \sqrt{2\pi} \int_{\mathrm{c}}^{\infty} \mathrm{e}^{\alpha \mathrm{x}} \varphi(-\beta \mathrm{x} + \delta) \mathrm{dx}$$

$$= -\frac{\sqrt{2\pi}}{\beta} \exp\{\frac{\alpha\delta}{\beta} + \frac{\alpha^2}{2\beta^2}\} \phi(\beta \mathrm{c} - \delta - \frac{\alpha}{\beta})$$

Solving it yields (B8), for $\mathrm{n} \geq -1$.

Finally, we sum the double exponential and the normal random variables

Proposition B.3.

Suppose $\{\xi_1, \xi_2, ...\}$ *is a sequence of i.i.d. exponential random variables with rate* $\eta > 0$, *and Z is a normal variable with distribution* $\mathrm{N}(0, \sigma^2)$. *Then for every* $\mathrm{n} \geq 1$, *we have: (1) The density functions are given by:*

$$\mathrm{f_{Z+\sum_{i=1}^{n} \xi_i}}(\mathrm{t}) = (\sigma\eta)^{\mathrm{n}} \frac{\mathrm{e}^{(\sigma\eta)^2/2}}{\sigma\sqrt{2\pi}} \mathrm{e}^{-\mathrm{t}\eta} \mathrm{Hh_{n-1}}(-\frac{\mathrm{t}}{\sigma} + \sigma\eta)$$

$$\mathrm{f_{Z-\sum_{i=1}^{n} \xi_i}}(\mathrm{t}) = (\sigma\eta)^{\mathrm{n}} \frac{\mathrm{e}^{(\sigma\eta)^2/2}}{\sigma\sqrt{2\pi}} \mathrm{e}^{-\mathrm{t}\eta} \mathrm{Hh_{n-1}}(\frac{\mathrm{t}}{\sigma} + \sigma\eta)$$

(2) The tail probabilities are given by

$$\mathrm{P}(\mathrm{Z}+\sum_{\mathrm{i}=1}^{\mathrm{n}}\xi_{\mathrm{i}}\geq \mathrm{x})=(\sigma\eta)^{\mathrm{n}}\frac{\mathrm{e}^{(\sigma\eta)^2/2}}{\sigma\sqrt{2\pi}}\mathrm{e}^{-\mathrm{t}\eta}\mathrm{I}_{\mathrm{n}-1}(\mathrm{x};-\eta,-\frac{1}{\sigma},-\sigma\eta)$$

$$\mathrm{P}(\mathrm{Z}-\sum_{\mathrm{i}=1}^{\mathrm{n}}\xi_{\mathrm{i}}\geq \mathrm{x})=(\sigma\eta)^{\mathrm{n}}\frac{\mathrm{e}^{(\sigma\eta)^2/2}}{\sigma\sqrt{2\pi}}\mathrm{e}^{-\mathrm{t}\eta}\mathrm{I}_{\mathrm{n}-1}(\mathrm{x};\eta,\frac{1}{\sigma},-\sigma\eta)$$

Proof. Case 1. The densities of $\mathrm{Z}+\sum_{\mathrm{i}=1}^{\mathrm{n}}\xi_{\mathrm{i}}$, *and* $\mathrm{Z}-\sum_{\mathrm{i}=1}^{\mathrm{n}}\xi_{\mathrm{i}}$. *We have*

$$\mathrm{f}_{\mathrm{Z}+\sum_{\mathrm{i}=1}^{\mathrm{n}}\xi_{\mathrm{i}}}(\mathrm{t})=\int_{-\infty}^{\infty}\mathrm{f}_{\sum_{\mathrm{i}=1}^{\mathrm{n}}\xi_{\mathrm{i}}}(\mathrm{t}-\mathrm{x})\mathrm{f}_{\mathrm{Z}}(\mathrm{x})\mathrm{dx}$$

$$=\mathrm{e}^{-\mathrm{t}\eta}(\eta^{\mathrm{n}})\int_{-\infty}\mathrm{t}\frac{\mathrm{e}^{\mathrm{x}\eta}(\mathrm{t}-\mathrm{x})^{\mathrm{n}-1}}{(\mathrm{n}-1)!}\frac{1}{\sigma\sqrt{2\pi}}\mathrm{e}^{-\mathrm{x}^2/(2\sigma^2)}\mathrm{dx}$$

$$=\mathrm{e}^{-\mathrm{t}\eta}(\eta^{\mathrm{n}})\mathrm{e}^{(\sigma\eta)^2/(2)}\int_{-\infty}\mathrm{t}\frac{(\mathrm{t}-\mathrm{x})^{\mathrm{n}-1}}{(\mathrm{n}-1)!}\frac{1}{\sigma\sqrt{2\pi}}\mathrm{e}^{-(\mathrm{x}-\sigma^2\eta)^2/(2\sigma^2)}\mathrm{dx}$$

Letting $\mathrm{y}=(\mathrm{x}-\sigma^2\eta)/\sigma$ *yields*

$$\mathrm{f}_{\mathrm{Z}+\sum_{\mathrm{i}=1}^{\mathrm{n}}\xi_{\mathrm{i}}}(\mathrm{t})=\mathrm{e}^{-\mathrm{t}\eta}(\eta^{\mathrm{n}})\mathrm{e}^{(\sigma\eta)^2/(2)}\sigma^{\mathrm{n}-1}$$

$$\times\int_{-\infty}^{\mathrm{t}/\sigma-\sigma\eta}\frac{(\mathrm{t}/\sigma-\mathrm{y}-\sigma\eta)^{\mathrm{n}-1}}{(\mathrm{n}-1)!}\frac{1}{\sqrt{2\pi}}\mathrm{e}^{-\mathrm{y}^2/2}\mathrm{dy}$$

$$=\frac{\mathrm{e}^{(\sigma\eta)^2/2}}{\sqrt{2\pi}}(\sigma^{\mathrm{n}-1}\eta^{\mathrm{n}})\mathrm{e}^{-\mathrm{t}\eta}\mathrm{Hh}_{\mathrm{n}-1}(-\mathrm{t}/\sigma+\sigma\eta)$$

because $(1/(\mathrm{n}-1)!)\int_{-\infty}\mathrm{a}(\mathrm{a}-\mathrm{y})^{\mathrm{n}-1}\mathrm{e}^{-\mathrm{y}^2/2}\mathrm{dy}=\mathrm{Hh}_{\mathrm{n}-1}(\mathrm{a})$. *The derivation of* $\mathrm{f}_{\mathrm{Z}+\sum_{\mathrm{i}=1}^{\mathrm{n}}\xi_{\mathrm{i}}}(\mathrm{t})$ *is similar.*

Case 2. $\mathrm{P}(\mathrm{Z}+\sum_{\mathrm{i}=1}^{\mathrm{n}}\xi_{\mathrm{i}}\geq \mathrm{x})$ *and* $\mathrm{P}(\mathrm{Z}-\sum_{\mathrm{i}=1}^{\mathrm{n}}\xi_{\mathrm{i}}\geq \mathrm{x})$. *From (B9), it is clear that*

$$\mathrm{P}(\mathrm{Z}+\sum_{\mathrm{i}=1}^{\mathrm{n}}\xi_{\mathrm{i}}\geq \mathrm{x})=\frac{(\sigma\eta)^{\mathrm{n}}\mathrm{e}^{(\sigma\eta)^2/2}}{\sigma\sqrt{2\pi}}\int_{\mathrm{x}}^{\infty}\mathrm{e}^{(-\mathrm{i}\eta)}\mathrm{Hh}_{\mathrm{n}-1}(-\frac{\mathrm{t}}{\sigma}+\sigma\eta)\mathrm{dt}$$

$$= \frac{(\sigma\eta)^{\mathrm{n}}\mathrm{e}^{(\sigma\eta)^2/2}}{\sigma\sqrt{2\pi}}\mathrm{I}_{\mathrm{n}-1}(\mathrm{x}; -\eta, -\frac{1}{\sigma}, -\sigma\eta)\mathrm{dt}$$

by (B6). We can compute $\mathrm{P}(\mathrm{Z} - \sum_{\mathrm{i}=1}^{\mathrm{n}} \xi_{\mathrm{i}} \geq \mathrm{x})$ *similarly.*

Theorem C.1. *Theorem With* $\pi_{\mathrm{n}} := \mathrm{P}(\mathrm{N}(\mathrm{t}) = \mathrm{n}) = \mathrm{e}^{-\lambda \mathrm{T}}(\lambda \mathrm{T})^{\mathrm{n}}/\mathrm{n}!$ *and* I_{n} *in Proposition* **??**. *, we have*

$$\mathrm{P}(\mathrm{Z}(\mathrm{T}) \geq \mathrm{a}) = \frac{\mathrm{e}^{(\sigma\eta_1)^2\mathrm{T}/2}}{\sigma\sqrt{2\pi\mathrm{T}}} \sum_{\mathrm{n}=1}^{\infty} \pi_{\mathrm{n}} \sum_{\mathrm{k}=1}^{\mathrm{n}} \mathrm{P}_{\mathrm{n,k}}(\sigma\sqrt{\mathrm{T}}\eta_1)^{\mathrm{k}} \times \mathrm{I}_{\mathrm{k}-1}(\mathrm{a} - \mu\mathrm{T}; -\eta_1, -\frac{1}{\sigma\sqrt{\mathrm{T}}}, -\sigma\eta_1\sqrt{\mathrm{T}})$$

$$+\frac{\mathrm{e}^{(\sigma\eta_2)^2\mathrm{T}/2}}{\sigma\sqrt{2\pi\mathrm{T}}} \sum_{\mathrm{n}=1}^{\infty} \pi_{\mathrm{n}} \sum_{\mathrm{k}=1}^{\mathrm{n}} \mathrm{Q}_{\mathrm{n,k}}(\sigma\sqrt{\mathrm{T}}\eta_2)^{\mathrm{k}}$$

$$\times \mathrm{I}_{\mathrm{k}-1}(\mathrm{a} - \mu\mathrm{T}; \eta_2, \frac{1}{\sigma\sqrt{\mathrm{T}}}, -\sigma\eta_2\sqrt{\mathrm{T}})$$

$$+\pi_0\phi(-\frac{\mathrm{a} - \mu\mathrm{T}}{\sigma\sqrt{\mathrm{T}}})$$

Proof by the decomposition (B2)

$$\mathrm{P}(\mathrm{Z}(\mathrm{T}) \geq \mathrm{a}) = \sum_{\mathrm{n}=0}^{\infty} \pi_{\mathrm{n}} \mathrm{P}(\mu\mathrm{T} + \sigma\sqrt{\mathrm{T}}\mathrm{Z} + \sum_{\mathrm{j}=1}^{\mathrm{n}} \mathrm{Y}_{\mathrm{j}} \geq \mathrm{a})$$

$$= \pi_0 \mathrm{P}(\mu\mathrm{T} + \sigma\sqrt{\mathrm{T}}\mathrm{Z} \geq \mathrm{a})$$

$$+ \sum_{\mathrm{n}=1}^{\infty} \pi_{\mathrm{n}} \sum_{\mathrm{k}=1}^{\mathrm{n}} \mathrm{P}_{\mathrm{n,k}} \mathrm{P}(\mu\mathrm{T} + \sigma\sqrt{\mathrm{T}}\mathrm{Z} + \sum_{\mathrm{j}=1}^{\mathrm{n}} \xi_{\mathrm{j}}^{+} \geq \mathrm{a})$$

$$+ \sum_{\mathrm{n}=1}^{\infty} \pi_{\mathrm{n}} \sum_{\mathrm{k}=1}^{\mathrm{n}} \mathrm{Q}_{\mathrm{n,k}} \mathrm{P}(\mu\mathrm{T} + \sigma\sqrt{\mathrm{T}}\mathrm{Z} - \sum_{\mathrm{j}=1}^{\mathrm{n}} \xi_{\mathrm{j}}^{-} \geq \mathrm{a})$$

The result now follows via (B11) and (B12) for $\eta_1 > 1$ *and* $\eta_2 > 0$.

APPENDIX D
DERIVATION OF THE Υ FUNCTION

We first decompose the sum of the double exponential random variables.

The memoryless property of exponential random variables yields $(\xi^+ - \xi^- | \xi^+ > \xi^-) =^{\mathrm{d}} \xi^+$ and $(\xi^+ - \xi^- | \xi^+ < \xi^-) =^{\mathrm{d}} -\xi^-$, thus leading to the conclusion that

$$\xi^+ - \xi^- = \left\{ \begin{array}{ll} \xi^+ & \text{with probability } \eta_2/(\eta_1+\eta_2) \\ -\xi^- & \text{with probability } \eta_1/(\eta_1+\eta_2) \end{array} \right\}.$$

because the probabilities of the events $\xi^+ > \xi^-$ and $\xi^+ < \xi^-$ are $\eta_2/(\eta_1+\eta_2)$ and $\eta_1/(\eta_1+\eta_2)$, respectively. The following proposition extends (B.1.)

Proposition B.1. For every $\mathrm{n} \geq 1$, we have the following decomposition

$$\sum_{\mathrm{i}=1}^{\mathrm{n}} \mathrm{Y_i} =^{\mathrm{d}} \left\{ \begin{array}{ll} \sum_{\mathrm{i}=1}^{\mathrm{k}} \xi_{\mathrm{i}}^+ & \text{with probability } \mathrm{P_{n,k}}, \mathrm{k} = 1,2,...,\mathrm{n} \\ -\sum_{\mathrm{i}=1}^{\mathrm{k}} \xi_{\mathrm{i}}^- & \text{with probability } \mathrm{Q_{n,k}}, \mathrm{k} = 1,2,...,\mathrm{n} \end{array} \right\}.$$

where $\mathrm{P_{n,k}}$ and $\mathrm{Q_{n,k}}$ are given by

$$\mathrm{P_{n,k}} = \sum_{\mathrm{i}=\mathrm{k}}^{\mathrm{n}-1} \binom{\mathrm{n}-\mathrm{k}-1}{\mathrm{i}-\mathrm{k}} \binom{\mathrm{n}}{\mathrm{i}} (\frac{\eta_1}{\eta_1+\eta_2})^{\mathrm{i}-\mathrm{k}} (\frac{\eta_2}{\eta_1+\eta_2})^{\mathrm{n}-\mathrm{i}} \mathrm{p}^{\mathrm{i}} \mathrm{q}^{\mathrm{n}-\mathrm{i}}$$

$$1 \leq \mathrm{k} \leq \mathrm{n}-1$$

$$\mathrm{Q_{n,k}} = \sum_{\mathrm{i}=\mathrm{k}}^{\mathrm{n}-1} \binom{\mathrm{n}-\mathrm{k}-1}{\mathrm{i}-\mathrm{k}} \binom{\mathrm{n}}{\mathrm{i}} (\frac{\eta_1}{\eta_1+\eta_2})^{\mathrm{n}-\mathrm{i}} (\frac{\eta_2}{\eta_1+\eta_2})^{\mathrm{i}-\mathrm{k}} \mathrm{p}^{\mathrm{n}-\mathrm{i}} \mathrm{q}^{\mathrm{i}}$$

$$1 \leq \mathrm{k} \leq \mathrm{n}-1, \mathrm{P_{n,n}} = \mathrm{p}^{\mathrm{n}}, \mathrm{Q_{n,n}} = \mathrm{q}^{\mathrm{n}}$$

and $\binom{0}{0}$ is defined to be one. Hence ξ_{i}^+ and ξ_{i}^- are i.i.d. exponential random variables with rates η_1 and η_2, respectively.

As a key step in deriving closed-form solutions for call and put options, this proposition indicates that the sum of the i.i.d. double exponential random variable can be written, in

distribution, as a randomly mixed gamma random variable. To prove Proposition B.1, the following lemma is needed.

Lemma B.1.

$$\sum_{i=1}^{n} \xi_i^+ - \sum_{i=1}^{n} \xi_i^-$$

$$=^d \left\{ \begin{array}{ll} \sum_{i=1}^{k} \xi_i & \text{with probability } \binom{n-k+m-1}{m-1} (\frac{\eta_1}{\eta_1+\eta_2})^{n-k} (\frac{\eta_2}{\eta_1+\eta_2})^{m}, k = 1, ..., n \\ -\sum_{i=1}^{l} \xi_i & \text{with probability } \binom{n-l+m-1}{n-1} (\frac{\eta_1}{\eta_1+\eta_2})^{n} (\frac{\eta_2}{\eta_1+\eta_2})^{m-l}, l = 1, ..., m \end{array} \right\}.$$

We prove it by introducing the random variables $A(n, m) = \sum_{i=1}^{n} \xi_i - \text{sum}_{j=1}^{m} \tilde{\xi}_j$ Then

$$A(n, m) =^d \left\{ \begin{array}{ll} A(n-1, m-1) + \xi^+ & \text{with probability } \eta_2/(\eta_1+\eta_2) \\ A(n-1, m-1) - \xi^- & \text{with probability } \eta_1/(\eta_1+\eta_2) \end{array} \right\}.$$

$$=^d \left\{ \begin{array}{ll} A(n, m-1) & \text{with probability } \eta_2/(\eta_1+\eta_2) \\ A(n-1, m) & \text{with probability } \eta_1/(\eta_1+\eta_2) \end{array} \right\}.$$

via B.1.. Now suppose horizontal axis that are representing the number of $\{\zeta_i^+\}$ and vertical axis representing the number of $\{\zeta_i^-\}$. Suppose we have a random walk on the integer lattice points. Starting from any point $(n, m), n, m \geq 1$, the random walk goes either one step to the left with probability $\eta_1/(\eta_1+\eta_2)$ or one step down with probability $\eta_2/(\eta_1+\eta_2)$, and the random walks stops once it reaches the horizontal or vertical axis. For any path from (n,m) to (k,0) , $1 \geq k \geq n$, it must reach (k,1) first before it makes a final move to (k,0). Furthermore, all the paths going from (n,m) to (k,1) must have exactly n-k lefts and m-1 downs, whence the total number of such paths is $\binom{n-k+m-1}{m-1}$. Similarly the total number of paths from (n,m) to (0,l) , $1 \geq l \geq m$, is $\binom{n-l+m-1}{n-1}$. Thus

$$A(n,m) =^{d} \left\{ \begin{array}{ll} \sum_{i=1}^{k} \xi_i & \text{with probability } \binom{n-k+m-1}{m-1}(\frac{\eta_1}{\eta_1+\eta_2})^{n-k}(\frac{\eta_2}{\eta_1+\eta_2})^{m}, k = 1, ..., n \\ -\sum_{i=1}^{l} \xi_i & \text{with probability } \binom{n-l+m-1}{n-1}(\frac{\eta_1}{\eta_1+\eta_2})^{n}(\frac{\eta_2}{\eta_1+\eta_2})^{m-l}, l = 1, ..., m \end{array} \right\}.$$

and the lemma is proven.

Now, let's prove the proposition B.1. By the same analogy used in Lemma B.1 to compute probability $P_{n,m}, 1 \geq k \geq n$, the probability weight assigned to $\sum_{i=1}^{k} \xi_i^+$ when we decompose $\sum_{i=1}^{k} Y_i$, it is equivalent to consider the probability of the random walk ever reach (k,0) starting from the point (i,n-i) being $\binom{n}{i}p^i q^{n-i}$. Note that the point (k,0) can only be reached from point (i,n-i) such that $k \geq i \geq n-1$, because the random walk can only go left or down, and stops once it reaches the horizontal axis. Therefore, for $1 \geq k \geq n-1$, (B3) leads to

$$P_{n,k} = \sum_{i=k} n-1 P(going from (i, n-i) to (k, 0)).P(starting from (i, n-i))$$

$$= \sum_{i=k}^{n-1} \binom{i+(n-i)-k-1}{(n-i)-1} \binom{n}{i} (\frac{\eta_1}{\eta_1+\eta_2})^{i-k} (\frac{\eta_2}{\eta_1+\eta_2})^{n-i} p^i q^{n-i}$$

$$= \sum_{i=k}^{n-1} \binom{n-k-1}{n-i-1} \binom{n}{i} (\frac{\eta_1}{\eta_1+\eta_2})^{i-k} (\frac{\eta_2}{\eta_1+\eta_2})^{n-i} p^i q^{n-i}$$

$$= \sum_{i=k}^{n-1} \binom{n-k-1}{i-k} \binom{n}{i} (\frac{\eta_1}{\eta_1+\eta_2})^{i-k} (\frac{\eta_2}{\eta_1+\eta_2})^{n-i} p^i q^{n-i}$$

Of course $P_{n,n} = p^n$. Similarly, we can compute $Q_{n,k}$:

$$Q_{n,k} = \sum_{i=k} n-1 P(going from (n-i, i) to (0, k)).P(starting from (n-i, i))$$

$$= \sum_{i=k}^{n-1} \binom{i+(n-i)-k-1}{(n-i)-1} \binom{n}{n-i} (\frac{\eta_1}{\eta_1+\eta_2})^{n-i} (\frac{\eta_2}{\eta_1+\eta_2})^{i-k} p^{n-i} q^{i}$$

$$= \sum_{i=k}^{n-1} \binom{n-k-1}{i-k} \binom{n}{i} (\frac{\eta_1}{\eta_1+\eta_2})^{n-i} (\frac{\eta_2}{\eta_1+\eta_2})^{i-k} p^{n-i} q^i$$

with $Q_{n,n} = q^n$. Incidentally, we have also got $\sum k = 1n(P_{n,k} + Q_{n,k}) = 1$

B.2. Let's develop now the results on Hh functions. First of all, note that $Hh_n(x) \to 0$, as $x \to \infty$, for $n \geq -1$; and $Hh_n(x) \to \infty$, as $x \to -\infty$, for $n \geq -1$; and $Hh_0(x) = \sqrt{2\pi}\phi(-x) \to \sqrt{2\pi}$, as $x \to -\infty$. Also, for every $n \geq -1$, as $x \to \infty$,

$$limHh_n(x)/\{\frac{1}{x^{n+1}} e^{-\frac{x^2}{2}}\} = 1$$

and as $x \to \infty$

$$Hh_n(x) = O(|x|^n)$$

Here (B4) is clearly true for $n = -1$, while for $n \geq 0$ note that as $x \to_\infty$,

$$Hh_n(x) = \frac{1}{n!} \int_x \infty (t-x)^n e^{-\frac{t^2}{2}} dt$$

$$\leq \frac{2^n}{n!} \int_{-\infty}^{\infty} |t|^n e^{-t^2} 2dt + \frac{2^n}{n!} \int -\infty\infty |x|^n e^{-t^2} 2dt = O(|x|^n)$$

For option pricing it is important to evaluate the integral $I_n(c; \alpha; \beta; \delta)$,

$$I_n(c; \alpha; \beta; \delta) = \int_c \infty e^{\alpha x} Hh_n(\beta x - \delta) dx, n \geq 0$$

for arbitrary constants α, c and β.

REFERENCES

Garfinkle, David, Horowitz, Gary T, and Strominger, Andrew. "Charged black holes in string theory." *Physical Review D* 43 (1991).10: 3140.

Green, Karen L. "A wrinkle in time." *comiXology* (2008).

L'engle, Madeleine. *A Wrinkle in Time: 50th Anniversary Commemorative Edition*, vol. 1. Macmillan, 2012.

Strickler, Howard D, Rosenberg, Philip S, Devesa, Susan S, Hertel, Joan, Fraumeni Jr, Joseph F, and Goedert, James J. "Contamination of poliovirus vaccines with simian virus 40 (1955-1963) and subsequent cancer rates." *Jama* 279 (1998).4: 292–295.

BIOGRAPHICAL SKETCH

This section is where your biographical sketch is typed in the bio.tex file. It should be in third person, past tense. Do not put personal details such as your birthday in the file. Again, to make a full paragraph you must write at least three sentences.